

Calculations of Electric Double-Layer Force and Interaction Free Energy between Dissimilar Surfaces

DREW MCCORMACK, STEVEN L. CARNIE, AND DEREK Y. C. CHAN¹

Department of Mathematics, University of Melbourne, Parkville, VIC 3052, Australia

Received March 14, 1994; accepted June 8, 1994

The nonlinear Poisson–Boltzmann theory is used to calculate the electrical double-layer force and interaction free energy between dissimilarly charged surfaces. For symmetric electrolytes, in addition to cases in which both surfaces maintain constant surface potential or constant surface charge during interaction, we also consider cases in which one surface maintains constant surface potential and the other maintains constant surface charge. We further present a general algorithm for calculating the double layer force and interaction free energy between surfaces with ionizable surface groups across electrolytes of any valence or composition. These results suggest interesting features of the double-layer interaction that can be observed by direct force measurement techniques. © 1995 Academic Press, Inc.

INTRODUCTION

Advances in the direct measurement of colloidal forces between particles and surfaces using a surface force apparatus (1) and an atomic force microscope allows the accurate determination of colloidal interactions between a variety of identical (2) and dissimilar surfaces (3). An important component of colloidal forces is the double-layer interaction that arises from the interaction between the charges on the surfaces of the particles across an intervening electrolyte solution. For interpreting experiments, it is important to have a method of calculating such forces with ease and precision.

In this paper, we consider the double-layer interaction between surfaces that may carry dissimilar charges or potentials across a symmetric electrolyte. We examine cases where (a) both surfaces maintain constant surface potentials, (b) both surfaces maintain constant surface charge densities, and (c) one surface maintains constant surface potential and the other maintains constant surface charge as the surfaces approach each other. We also advance a general numerical method for solving the Poisson–Boltzmann to calculate the interaction between flat plates across a electrolyte of arbitrary valence and ionic composition. This method can be readily applied to surfaces with constant surface potential or charge as well as to surfaces bearing ionizable groups.

The theoretical basis of our calculations of the double-layer interaction is the nonlinear Poisson–Boltzmann equation (4). We shall consider the interaction between parallel plates from which we can obtain the interaction between surfaces of different curvatures using the Deryaguin construction (5), provided all radii of curvature are large compared to the characteristic Debye length of the electrolyte.

Verwey and Overbeek (4) had considered in detail the interaction between identical plates under constant surface potential. The interaction between identical flat plates at constant surface potential and constant surface charge under the nonlinear Poisson–Boltzmann theory has also been studied by Honig and Mul (6), who provided numerical tabulations of the force and interaction free energy. There have also been studies on the effects of constant charge boundary conditions based on the linearized version of the Poisson–Boltzmann equation (7, 8).

The study of the double-layer interaction between dissimilar surfaces is more complicated than the case of identical surfaces as there is now the possibility of surfaces having surface potentials and surface charge densities of different sign and magnitude. Due to this complexity, the result of Hogg *et al.* (9) for the interaction between two dissimilar surfaces at constant potential has been used in many applications. This theory is based on the Deryaguin construction of the interaction between parallel plates determined according to the linearized versions of the Poisson–Boltzmann equation that is appropriate for low surface potentials (see also (11, 12)). Parsegian and Gingell (13) also used the linearized versions of the Poisson–Boltzmann equation to study the interaction between dissimilar plates under either constant potential or constant charge conditions and gave a general account of how the various combinations of signs and magnitudes of the surface charge densities and potentials can affect the variations of the interaction with separation. This work has recently been extended to boundary conditions appropriate to the case in which the ionizable surface groups can dissociate during particle interaction, whereby neither the surface potentials nor the surface charges remain constant during interaction (14, 23, 24).

¹ To whom correspondence should be addressed.

A clear and detailed account of the interaction between dissimilarly charged surfaces across a symmetric electrolyte has been given by Devereux and de Bruyn (15). Their work is based on the nonlinear Poisson–Boltzmann equation and extensive numerical tabulations of the force and interaction free energy per unit area between the flat plates interacting under constant surface potentials were provided. Unfortunately, some results in these tables at extreme parameter limits contain large errors. Bell and Peterson (16) and Ohshima (17) studied the more general case of dissimilar surfaces interacting under constant charge. The interaction between spheres has also been constructed from these flat plate results using the Deryaguin construction (6, 16).

This paper aims to draw together these diverse results into a coherent whole. A general method for visualizing the qualitative forms of the variation of the force per unit area between flat plates as well as the variation of the surface potentials and surface charges with separation will be also given. General physical principles that can be used to explain the results of our calculations will be discussed. Our numerical implementations of these calculations are sufficiently responsive that it is feasible to perform very accurate calculations of double-layer interactions on desktop computers so that the use of approximate formulae are no longer justified unless an approximate analytic expression is required.²

In the next section, we set up the Poisson–Boltzmann problem of interacting parallel plates for dissimilar surfaces across a symmetric electrolyte. Next, we introduce a simple graphical method which can be used to predict the qualitative features of the force per unit area vs separation curve for dissimilar interacting surfaces without doing any computations. Asymptotic formulae for the force per unit area are also given. Then we list different equivalent expressions for the double-layer free energy and note that some are more suited for yielding higher precision numerical results. This is followed by numerical results for dissimilar surfaces interacting across a symmetric electrolyte. The surfaces can maintain both constant potential or constant charge or a mix of constant potential and constant charge. Thereafter, we present a general method of calculating the interaction free energy between dissimilar surfaces across a general multivalent, multicomponent electrolyte. This method can easily handle surfaces bearing ionizable surface groups which give rise to nonlinear boundary conditions.

A glossary of symbols is included at the end of the paper.

SOLUTION FOR SYMMETRIC ELECTROLYTE

We first summarize the main results that form the basis of our calculations of double-layer interaction across symmetric electrolytes. For easier reference to earlier work, we

² Details of the numerical implementations of these calculation are available from the authors. E-mail: dyc@mundoe.maths.mu.oz.au

shall, where possible, use the notation of Devereux and de Bruyn (6).

The one-dimensional nonlinear Poisson–Boltzmann equation for the mean electrostatic potential, $\psi(x)$, valid for a symmetric $\nu:\nu$ electrolyte present between two charged planar surfaces located at a distance d apart can be written in the nondimensional form

$$\frac{d^2 y(\xi)}{d\xi^2} = \sinh y(\xi). \quad [1]$$

Here $y = (e\nu\psi/k_B T)$ is the potential scaled by the thermal potential ($k_B T/e\nu$), with k_B being the Boltzmann constant, T the absolute temperature, and e the protonic charge. The coordinate, x , normal to the surface is related to the scaled variable $\xi = \kappa x$ by the Debye screening length $\kappa^{-1} = (8\pi n\nu^2 e^2/\epsilon k_B T)^{-1/2}$, where ϵ is the dielectric constant of the solvent and n is the number density of ions in the bulk electrolyte. We place one surface at the origin, $\xi = 0$, while the other surface is at $\xi = \kappa d$ (see Fig. 1).

Since the force and interaction free energies in a symmetric electrolyte remain unchanged if we negate the signs of the potential or charge on both surfaces, we can, without loss of generality, arrange the surface potential at $\xi = 0$ and at $\xi = \kappa d$ to be y_0 and y_d , respectively, with y_0 always positive and greater than y_d which may have either sign. Hereafter, we assume quite generally that

$$y_0 > |y_d| > 0. \quad [2]$$

We note that y_0 and y_d are simply the values of the potentials on the surfaces when they are a distance d apart. For constant potential boundary conditions these will, of course, be independent of the plate separation. For constant charge surfaces these will vary as the separation varies and their values

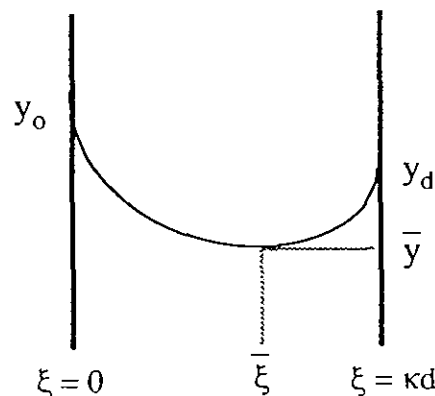


FIG. 1. Schematic representation of the nondimensional potential profile between two charged plates with a potential minimum \bar{y} located at $\bar{\xi}$. The coordinate system is constructed to ensure $y_0 \geq |y_d| \geq 0$, by changing the signs of both surfaces, if necessary.

are determined by the electrostatic boundary condition that relates the derivative of the potential to the surface charge density σ

$$\frac{d\psi}{dx} = -\frac{4\pi\sigma_0}{\epsilon}, \text{ at } x = 0; \quad \frac{d\psi}{dx} = \frac{4\pi\sigma_d}{\epsilon}, \text{ at } x = d. \quad [3]$$

In terms of the scaled variables, these boundary conditions become

$$\frac{dy}{d\xi} = -s_0, \text{ at } \xi = 0; \quad \frac{dy}{d\xi} = s_d, \text{ at } \xi = \kappa d, \quad [4]$$

where the scaled surface charge density s is defined by

$$s_i = \frac{4\pi e\nu}{\kappa\epsilon k_B T} \sigma_i, \quad i = 0 \text{ or } d. \quad [5]$$

The Poisson–Boltzmann Eq. [1] can be integrated once to give

$$\left(\frac{dy}{d\xi}\right) = \pm\sqrt{2 \cosh y + C}, \quad [6]$$

where the constant of integration C is yet to be determined. However, if we evaluate [6] at $\xi = 0$ or κd and apply the boundary conditions given by Eq. [4], we have

$$s_0^2 = 2 \cosh y_0 + C, \quad [7a]$$

$$s_d^2 = 2 \cosh y_d + C. \quad [7b]$$

These are two relations between the surface potential and the surface charge on each surface in terms of the integration constant C which is itself a function of the plate separation, d . In general, both the potential and the charge may vary as the plate separation changes, but their values must be related by [7]. At large separations ($d \rightarrow \infty$) both y and $(dy/d\xi)$ must vanish, so the constant, by Eq. [6], becomes

$$C \rightarrow -2 \text{ as } d \rightarrow \infty, \quad [8]$$

whereupon we have the result

$$s_{0\infty} = 2 \sinh(y_{0\infty}/2); \quad s_{d\infty} = 2 \sinh(y_{d\infty}/2), \quad [9]$$

as $d \rightarrow \infty$. Equation [9] relates the potentials and charge densities for the plates in isolation, as denoted by the subscript ∞ .

The force per unit area acting between the plates is given by a sum of a repulsive osmotic term and an attractive Maxwell stress contribution

$$P = 2nk_B T [\cosh(e\nu\psi(x)/kT) - 1] - \frac{\epsilon}{8\pi} \left(\frac{d\psi(x)}{dx}\right)^2, \quad [10]$$

where positive values of P correspond to repulsion between the plates. This expression for P is also independent of x so that we can evaluate [10] at $x = 0$ and $x = d$ to give two equivalent results,

$$P = 2nk_B T \{ [\cosh(y_0) - 1] - \frac{1}{2}s_0^2 \} \\ = -2nk_B T \{ \frac{1}{2}(C + 2) \}, \quad x = 0 \quad [11a]$$

$$P = 2nk_B T \{ [\cosh(y_d) - 1] - \frac{1}{2}s_d^2 \} \\ = -2nk_B T \{ \frac{1}{2}(C + 2) \}, \quad x = d, \quad [11b]$$

where the second equalities in both parts of [11] follow from Eq. [7]. We see that the force acting between the plates is directly related to the integration constant C which itself is a function of the plate separation, d . For $C < -2$ (or $C > -2$), Eq. [11] will give $P > 0$ (or $P < 0$), which corresponds to a repulsive (attractive) force per unit area between the plates.

The result in [11] is important in another respect. In addition to providing a natural definition of a nondimensional force per unit area

$$p \equiv P/2nk_B T = -\frac{1}{2}(C + 2), \quad [12]$$

it can be rearranged to give the results

$$p = -\frac{1}{2}(C + 2) = 2 \sinh^2(y_0/2) - \frac{1}{2}s_0^2 \quad [13a]$$

$$= 2 \sinh^2(y_d/2) - \frac{1}{2}s_d^2, \quad [13b]$$

which allow us to visualize the qualitative variations of the force, surface charge, and surface potential as the plates approach each other. As the separation between the plates changes the potential and charge on *each* plate must be related to the integration constant C , or equivalently the force per unit area, by [13a] or [13b]. Furthermore, the potentials and charges on both plates must also be interrelated by the two parts of [13]. We shall return to this point in the next section.

The form of the second integral of [6] depends on the sign and magnitude of the integration constant C as well as the sign of the surface potential y_d . There are three distinct cases: (I) $C < -2$, (II) $-2 < C < 2$, and (III) $C > 2$. Case I corresponds to repulsive interactions, while cases II and III correspond to attractive interactions. The integrals of Eq. [6] given by Devereux and de Bruyn (15) express the position in terms of the potential using elliptic integrals. However, we have also give expressions for the potential as functions of position in terms of Jacobi elliptic functions. These results are summarized in Table 1. We briefly comment on the results of each case separately.

TABLE 1
Solutions of the Poisson-Boltzmann Equation for Different Values of the Integration Constant C

(I) $C \leq -2$

(a) $\xi = 2k^{1/2}\{F(k, \phi) - F(k, \phi_0)\}$, $0 \leq \xi \leq \bar{\xi}$, $y'(\xi) < 0$, $C \leq -2$.

(b) $\xi = 2k^{1/2}\{2K(k) - F(k, \phi) - F(k, \phi_0)\}$, $\bar{\xi} \leq \xi \leq \kappa d$, $y'(\xi) > 0$, $C \leq -2$.

(c) $y(\xi) = \bar{y} - 2 \log\left(\frac{\sin \phi_0 \operatorname{cn}(k; z) \operatorname{dn}(k; z) + \cos \phi_0 (1 - k^2 \sin^2 \phi_0)^{1/2} \operatorname{sn}(k; z)}{1 - k^2 \sin^2 \phi_0 \operatorname{sn}^2(k; z)}\right)$, $C < -2$.

(d) $C = -2 \cosh \bar{y}$; $k = \exp(-\bar{y})$; $\phi = \sin^{-1}(\exp([\bar{y} - y]/2))$; $\phi_0 = \sin^{-1}(\exp([\bar{y} - y_0]/2))$; $\bar{y} = y(\xi)$; $z = \frac{\xi}{2k^{1/2}}$.

(II) $-2 \leq C \leq 2$

(a) $\xi = F(k, \phi) - F(k, \phi_0)$, $y > 0$, $-2 \leq C \leq 2$.

(b) $\xi = 2K(k) - F(k, \phi) - F(k, \phi_0)$, $y < 0$, $-2 \leq C \leq 2$.

(c) $y(\xi) = \pm 2 \cosh^{-1}\left(\frac{1 - k^2 \sin^2 \phi_0 \operatorname{sn}^2(k; \xi)}{\sin \phi_0 \operatorname{cn}(k; \xi) \operatorname{dn}(k; \xi) + \cos \phi_0 (1 - k^2 \sin^2 \phi_0)^{1/2} \operatorname{sn}(k; \xi)}\right)$, $-2 \leq C \leq 2$.

(d) $k = \left(\frac{2 - C}{4}\right)^{1/2}$; $\phi = \sin^{-1}\left(\frac{1}{\cosh(y/2)}\right)$; $\phi_0 = \sin^{-1}\left(\frac{1}{\cosh(y_0/2)}\right)$.

(III) $C \geq 2$

(a) $\xi = (2/b)\{F(k, \phi_0) - F(k, \phi)\}$, y any sign, $C \geq 2$.

(b) $y(\xi) = 2 \log\left(\frac{1}{b} \tan\left(\sin^{-1}\left(\frac{\sin \phi_0 \operatorname{cn}(k; z) \operatorname{dn}(k; z) - \cos \phi_0 (1 - k^2 \sin^2 \phi_0)^{1/2} \operatorname{sn}(k; z)}{1 - k^2 \sin^2 \phi_0 \operatorname{sn}^2(k; z)}\right)\right)\right)$, $C \geq 2$.

(c) $C = b^2 + b^{-2}$; $k = \sqrt{1 - b^{-4}}$, $b \geq 1$; $\phi = \tan^{-1}(b \exp(y/2))$; $\phi_0 = \tan^{-1}(b \exp(y_0/2))$; $z = b\xi/2$.

(IV) $C = -2$

(a) $\xi = \log\left(\frac{\tanh(y_0/4)}{\tanh(y/4)}\right)$, $C = -2$.

(b) $y(\xi) = 2 \log\left(\frac{1 + e^{-\xi} \tanh(y_0/4)}{1 - e^{-\xi} \tanh(y_0/4)}\right)$, $C = -2$.

(V) $C = 2$

(a) $\xi = 2(\tan^{-1}(\exp(y_0/2)) - \tan^{-1}(\exp(y/2)))$, $C = 2$.

(b) $y(\xi) = 2 \log\left(\frac{\exp(y_0/2) - \tan(\xi/2)}{1 + \exp(y_0/2) \tan(\xi/2)}\right)$, $C = 2$.

Note. All results of the inverse trigonometric functions are in the first quadrant. The elliptic integrals $F(k, \phi)$, $K(k)$ and the Jacobi elliptic functions $\operatorname{sn}(k; u)$, $\operatorname{cn}(k; u)$, and $\operatorname{dn}(k; u)$ are defined in Appendix 1. See text for definition of symbols.

(I) $C \leq -2$

In this case, the force between the plates is repulsive and the curve $y(\xi)$ has a minimum at $\xi = \bar{\xi}$ where the potential is $y(\bar{\xi}) = \bar{y} \geq 0$, and we may write

$$C = -2 \cosh \bar{y}. \tag{14}$$

Depending on the values of y_0 , y_d and the separation κd , this potential minimum may be located outside the plates, i.e., $\bar{\xi} > \kappa d$ or located in between the plates, i.e., $0 \leq \bar{\xi} \leq \kappa d$. In the first case, when $\bar{\xi} > \kappa d$, the slope of the curve $y(\xi)$ is always negative and one should choose the negative square root in [6]. The resulting integral is entry (Ia) in Table 1. On the other hand, if the potential minimum is located between the plates, i.e., $0 \leq \bar{\xi} \leq \kappa d$, then the entry (Ia) in Table 1 will still be applicable when ξ is in the range $0 \leq \xi \leq \bar{\xi}$; but when ξ is in the range $\bar{\xi} \leq \xi \leq \kappa d$, where the slope of

$y(\xi)$ is positive, one should choose the positive square root in [6] which then leads to entry (Ib) in Table 1. Thus if the potentials y_0 and y_d are known then either (Ia) or (Ib) in Table 1, where appropriate, should be used to determine the integration constant C by setting $\xi = \kappa d$ and $y = y_d$. If instead the surface charges are specified, the surface potentials may be determined with the aid of [7]. Once the constant C is found, the force between the plates may be determined from [12]. The explicit expression of the potential $y(\xi)$ given in entry (Ic) in Table 1 applies for $C < -2$, irrespective of the sign of $dy(\xi)/d\xi$.

(II) $-2 \leq C \leq 2$

In this case, the curve $y(\xi)$ has no minimum so the slope is always negative and, from Eq. [11], the force between the plates is attractive. Therefore, Eq. [6], with the choice of negative square root should then be integrated. The final

results, depending on whether $y(\xi)$ is positive or negative, are given in entries (IIa) and (IIb) in Table 1. The expressions for $y(\xi)$ are given in entry (IIc) of Table 1. The description on how to find the integration constant C given in Case I also apply here.

(III) $C \geq 2$

This case also corresponds to an attractive force, see Eq. [11]. However, since the curve $y(\xi)$ has no minimum, Eq. [6], with the negative square root, should be integrated. The result is given in entry (IIIa) with the corresponding expression for $y(\xi)$ in (IIIb) in Table 1.

Given the plate separation, κd , and values of the surface potentials y_0 and y_d as known constants or in terms of the surface charge via Eq. [7], we can solve the appropriate equation in Table 1 to determine the integration constant C and hence the force per unit acting between the plates. We note that the force at separation κd depends only on the values of the potentials y_0 and y_d at that separation; it does not depend on whether the surfaces are held at constant potential or constant charge or how the potentials may change when the separation changes.

In order to decide which equation in Table 1 to use to find C , we note that the solutions that are valid on either side of the values, $C = -2$ and 2 , should match up. The integral of Eq. [6] at $C = -2$ and $C = 2$ are also given in Table 1. Thus by setting $y = y_d$ we can calculate those critical values of (κd) at which we need to switch from using one solution to another. For dissimilar surfaces, we also need to know at what separation the surface potentials may change sign. We can determine this by a simple graphical method that we shall discuss next.

GRAPHICAL ANALYSIS OF THE INTERACTION

In this section, we demonstrate how we can obtain general qualitative information about variations of the force, surface potentials, and surface charges with separation without solving any equations. We recall that Eq. [13] relates the non-dimensional force per unit area, p , to the surface potential and surface charge. This result forms the basis of a simple graphical method for determining the variation of the force, surface potentials, and surface charges with separation. We can regard the non-dimensional surface charge, s , as a function of the surface potential, y_s , which we denote by $s(y_s)$ and plot the curves $\{2 \sinh^2(y_s/2)\}$ and $\{\frac{1}{2}s^2(y_s)\}$ on the same set of axes as functions of the surface potential y_s . As shown in Fig. 2, a constant potential surface is represented by a vertical line, while a constant charge surface is represented by a horizontal line. At any separation, the surface potential and surface charge must correspond to a point on the $s(y_s)$ curve which we can regard as the "equation of state" of the surface in terms of the coordinate (y_s, s) and the diagram in Fig. 2 represents the "phase space" of the

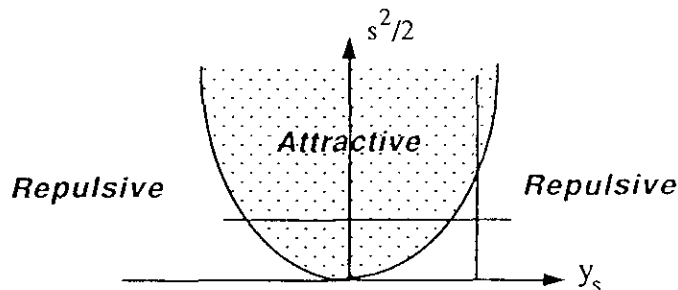


FIG. 2. Schematic representation of the curve $\{2 \sinh^2(y_s/2)\}$ as a function of the surface potential, y_s . The vertical line is the curve for the non-dimensional surface charge, s , when a surface is at constant potential. The horizontal line is the curve for the nondimensional surface charges, s , when a surface is at constant charge.

interacting system. Although the axes in Fig. 2 are $\frac{1}{2}s^2$ and y_s , we can, without any confusion, refer to the state point as (y_s, s) to avoid the cumbersome notation. Whenever the point (y_s, s) lies *above* the curve $\{2 \sinh^2(y_s/2)\}$, the non-dimensional force per unit area, p , will be negative, which corresponds to an attractive force—this is indicated by the shaded region in Fig. 2. For points (y_s, s) that lie *below* the curve $\{2 \sinh^2(y_s/2)\}$, the force will be positive which corresponds to repulsion. The *vertical distance* between the curve $\{2 \sinh^2(y_s/2)\}$ and the point (y_s, s) is the non-dimensional force per unit area, p .

If the surface potentials on the plates are $y_{0\infty}$ and $y_{d\infty}$ when the plates are far apart ($d \rightarrow \infty$) the force will be zero so the corresponding surface charges can be found by setting $p = 0$ in [13], which leads to [9] for the relation between the surface potentials $y_{0\infty}$ and $y_{d\infty}$ and the surface charge densities $s_{0\infty}$ and $s_{d\infty}$. In other words, the points $(y_{0\infty}, s_{0\infty})$ and $(y_{d\infty}, s_{d\infty})$ will be where the curves $s_0(y_0)$ and $s_d(y_d)$ intersect the curve $\{2 \sinh^2(y_s/2)\}$. Furthermore, the relative positions of the curves $s_0(y_0)$, $s_d(y_d)$ and the curve $\{2 \sinh^2(y_s/2)\}$ will control how the force, surface potential, or surface charge will vary as the plate separation changes. We shall study the cases in which (a) both plates are moved together at constant potential, (b) both plates are moved together at constant charge, and (c) one plate is held at constant potential and the other at constant charge.

(a) Both Plates at Constant Potential

The charge–potential curves for this case is given in Fig. 3, where we have the possibility of the surfaces having the same (Fig. 3a) or different signs (Fig. 3b) at infinite separation.

(i) Potentials with Same Signs

When surfaces having unequal potentials of the same sign at infinite separation are moved together, both surface charges will fall in magnitude, the (y, s) coordinate of each

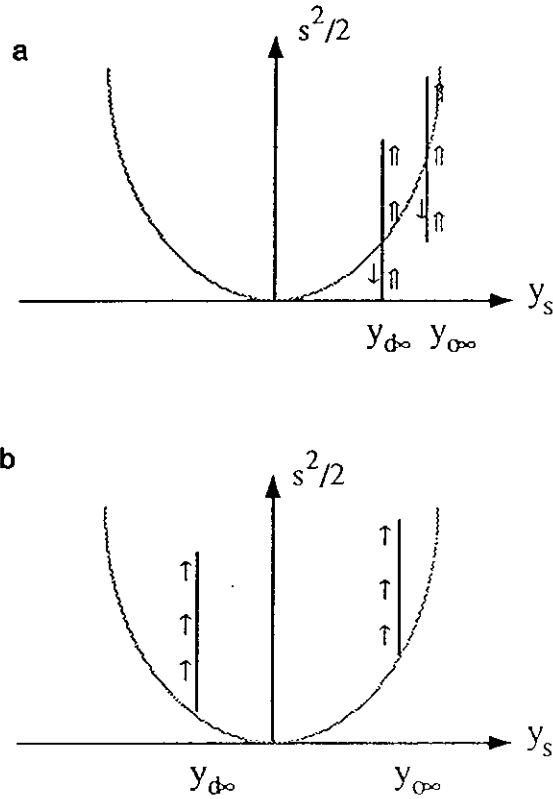


FIG. 3. Evolution of the state points (y, s) for two interacting constant potential surfaces. The arrows indicate the movement of the state points as the separation decreases from infinity—(a) surfaces have the same (positive) sign at infinite separation; (b) surfaces have opposite signs at infinite separation.

surface will move along the $s(y)$ curves in the direction of the single arrows indicated in Fig. 3a, into the repulsive region of phase space (see Fig. 2), where the force will be repulsive ($C < -2$). The potential will be determined by Eq. [1b] in Table 1 as there will be a potential minimum with $0 \leq \bar{\xi} \leq \kappa d$. This continues until the surface with the smaller potential reaches zero charge ($s_d = 0$). At this point the nondimensional repulsive force per unit area has reached a maximum repulsive value of

$$P = P_{\max} = -(2nk_B T) \frac{1}{2} (C_{\max} + 2) \\ = (2nk_B T) \{2 \sinh^2(y_{d\infty}/2)\}, \quad [15]$$

corresponding to a most negative value of $C = C_{\max} < -2$. We may use Eqs. [14]–[16] to determine the plate separation, d_{\max} say, at which this will occur. At this point, the potential minimum $\bar{v} = y_{d\infty}$ and it is located at $\bar{\xi} = \kappa d$. As the plate separation is reduced to less than d_{\max} , the surface charge on the plates will begin to increase in magnitude (double arrows in Fig. 3a) and the plate at $x = d$ will now have a surface charge of *opposite* sign to $s_{d\infty}$ —and the force will become less repulsive. The potential will no longer have

a minimum in $(0, \kappa d)$ so the potential will now be given by Eq. [1a] in Table 1. When the (y, s) coordinate of each surface returns to the curve $\{2 \sinh^2(y_s/2)\}$, the force will have decreased to zero ($C = -2$). The separation at which this occurs can be found from Eq. [IVa] in Table 1. As the separation is further reduced, the (y, s) coordinates will move into the attractive region (see Fig. 2) ($-2 \leq C \leq 2$, Eq. [IIa] in Table 1) and remain there as $d \rightarrow 0$. The force now becomes increasingly more negative. As the separation decreases further, the system will then move into the regime $C \geq 2$, Eq. [IIIa] in Table 1. In the limit $d \rightarrow 0$, the attractive Maxwell stress term in [10] dominates and the force per unit area diverges like

$$P \rightarrow -\frac{\epsilon}{8\pi} \left(\frac{\psi_{0\infty} - \psi_{d\infty}}{d} \right)^2, \quad d \rightarrow 0. \quad [16]$$

In the special case of identical surfaces, the force is always positive and increases with decreasing separation until it reaches P_{\max} at zero separation.

(ii) Potentials with Opposite Signs

When the surfaces have opposite signs, the force is always attractive ($C > -2$) and the (y, s) coordinates always remain in the attractive region (Figs. 2 and 3b). The force is a monotonical decreasing function of separation. At small separations, the form of the force is again given by [16]. The case $-2 \leq C \leq 2$, Eq. [IIa] in Table 1, will give the potential distribution at large separations; but when the separation reaches the critical value given by [Va] in Table 1 with $y = y_d$, the case $C \geq 2$ given by Eq. [IIIa] in Table 1, will apply.

(b) Both Plates at Constant Charge

In this case, we still characterize the surfaces by their potentials at infinite separation $y_{0\infty}$ and $y_{d\infty}$, which are related to the fixed surface charge densities σ_0 and σ_d by Eq. [9]. As mentioned earlier, the surfaces are rearranged, without loss of generality, to ensure $y_{0\infty} > |y_{d\infty}| > 0$. The charge-potential curves for this case are shown in Fig. 4 for surfaces having the same (Fig. 4a) or different signs (Fig. 4b) at infinite separation.

(i) Charges with Same Signs

When both surfaces have the same sign at large separations, the interaction is always repulsive ($C < -2$) and there will always be a potential minimum \bar{y} in the range $0 \leq \bar{\xi} \leq \kappa d$. The movement of the (y, s) coordinate of each surface is illustrated in Fig. 4a. In the limit $d \rightarrow 0$, the force per unit area diverges like (25)

$$P \rightarrow \frac{k_B T}{e} \left(\frac{\sigma_0 + \sigma_d}{d} \right), \quad d \rightarrow 0, \quad [17]$$

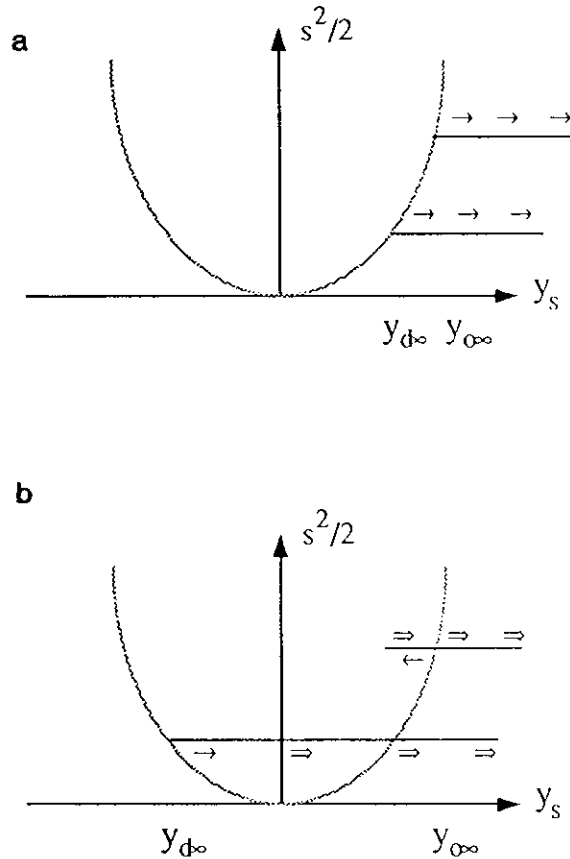


FIG. 4. Evolution of the state points (y, s) for two interacting constant charge surfaces. The arrows indicate the movement of the state points as the separation decreases from infinity—(a) surfaces have the same (positive) sign at infinite separation; (b) surfaces have opposite signs at infinite separation.

which is the pressure exerted by $[(\sigma_0 + \sigma_d)/e]$ ideal molecules per unit area confined between the plates at a separation d apart.

(ii) Charges with Opposite Signs

With surfaces of opposite sign at large separations, the movement of the (y, s) coordinate of each surface is illustrated in Fig. 4b. At large separations, the force is attractive and the potential of both surfaces falls in magnitude with decreasing separation until the surface potential, y_d , on the originally negative surface reaches zero. At this point the force per unit area reaches an attractive minimum given by

$$P = P_{\min} = -(2nk_B T) \frac{1}{2} (C_{\min} + 2) = -2\pi\epsilon\sigma_d^2. \quad [18]$$

At the same point, the potential, y_0 , on the other surface has also reached a minimum value but remains positive. As the separation further decreases, y_d becomes positive and together with y_0 begins to increase in magnitude (indicated by double arrows in Fig. 4b). The force also becomes less negative and

will reach zero (corresponding to $C = -2$) at the points where the two charge curves intersect with the curve $\{2 \sinh^2(y_s/2)\}$, at y_0 and $|y_d|$. The separation at which this occurs can be found from Eq. [IVa] in Table 1 by setting $y = |y_d|$. Thereafter, the (y, s) coordinates of the surfaces will move into the repulsive region (see Fig. 2) and the force will stay positive or repulsive and remain so as $d \rightarrow 0$. In this limit, the force per unit area diverges like

$$P \rightarrow \frac{k_B T}{e} \left(\frac{\sigma_0 + \sigma_d}{d} \right), \quad d \rightarrow 0. \quad [19]$$

In the case where the surface charges are exactly equal and opposite, $\sigma_0 = -|\sigma_d|$, the force will be monotonically attractive for all separations with the force attaining the minimum value given by Eq. [18] at $d = 0$. In this case, both surface potentials will approach zero monotonically as $d \rightarrow 0$.

(c) One Plate at Constant Charge and the Other at Constant Potential

Here we consider the case in which one surface is held at constant potential and the other at constant charge. Again the surfaces can be characterized in terms of their surface potentials at infinite separation: $y_{0\infty}$ and $y_{d\infty}$, arranged so that $y_{0\infty} \geq |y_{d\infty}| \geq 0$. There are four distinct cases to consider depending on whether $y_{0\infty}$ and $y_{d\infty}$ have the same or opposite signs and also whether y_0 is at constant potential or constant charge. The movement of the (y, s) coordinate of each surface for these four cases as the plate separation changes is shown in Figs. 5a–5d.

(i) Surfaces with Same Signs

(1) *Surface with higher potential is at constant charge.* When the surface at $\xi = 0$, arranged to have a higher potential at infinite separation, is held at constant charge the movements of the (y, s) coordinates of each surface with decreasing plate separation is shown in Fig. 5a. As the separation decreases from infinity, the surface charge on the constant potential surface will fall, but the surface potential on the constant charge surface will rise. Thus, the force is repulsive at large separations and has a repulsive force maximum when the surface charge on the constant potential plate at $\xi = \kappa d$ falls to zero. The magnitude of this force maximum is

$$P = P_{\max} = -(2nk_B T) \frac{1}{2} (C_{\max} + 2) \\ = (2nk_B T) \{ 2 \sinh^2(y_{d\infty}/2) \} = \frac{2\pi\sigma_{d\infty}^2}{\epsilon}. \quad [20]$$

The separation d_{\max} at which this force maximum occurs can be found from Eqs. [7] and [14] and the equations in

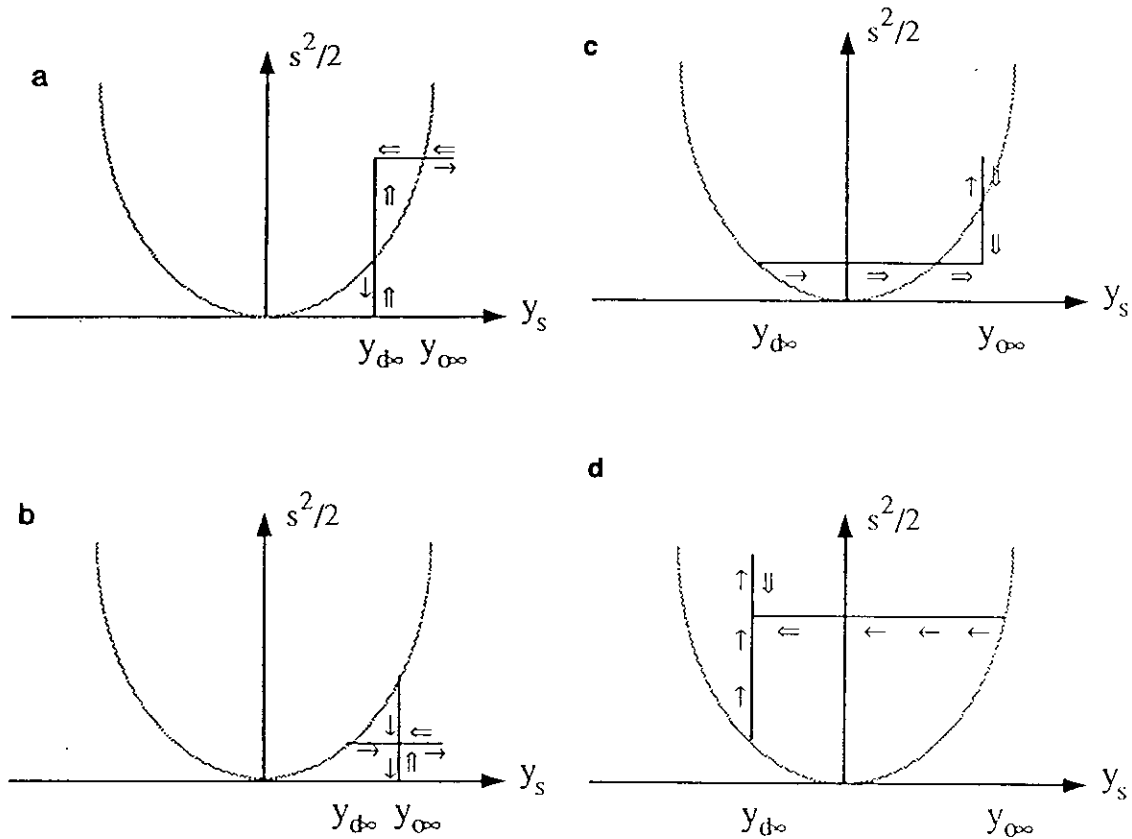


FIG. 5. Evolution of the state points (y, s) for a constant potential surface interacting with a constant charge surfaces. The arrows indicate the movement of the state points as the separation decreases from infinity—(a, b) surfaces have the same (positive) sign at infinite separation, (c, d) surfaces have opposite signs at infinite separation. In cases (a) and (d), the surface with the higher potential at infinite separation is at constant charge and in cases (b) and (d), the surface with the higher potential at infinite separation is at constant potential.

section I of Table 1, with $C = C_{\max}$ and $y = 0$. For $d < d_{\max}$, the force will decrease and eventually become attractive as shown by the double arrows in Fig. 5a. At $d = 0$, the potentials on the plates will both be equal to $y_{d\infty}$, while the charge on the surfaces will be equal and opposite with magnitude σ_0 . Therefore at $d = 0$, the force has a negative value given by

$$P = (2nk_B T) [2 \sinh^2(y_{d\infty}/2)] - \frac{2\pi\sigma_0^2}{\epsilon} = -\frac{2\pi(\sigma_0^2 - \sigma_d^2)}{\epsilon}$$

$$= -(2nk_B T) \{2 \sinh^2(y_{0\infty}/2) - 2 \sinh^2(y_{d\infty}/2)\}. \quad [21]$$

(2) *Surface with higher potential is at constant potential.* When the surface at $\xi = 0$, which is arranged to have a higher potential at infinite separation, is held at constant potential (Fig. 5b), the force will be repulsive at all separations. As the separation decreases from infinity, the surface charge on the constant potential surface will fall, but the surface potential on the constant charge surface will rise. Eventually, a separation will be reached when the two surface potentials are equal—this coincides with

the point at which the potential and charge curves of the two surfaces intersect. At smaller separations we need to relocate the origin of the coordinate system to the other surface as all equations we have derived for the potential as a function of position assume that the potential at the origin is higher than the potential at $\xi = \kappa d$. The force has a repulsive maximum when the surface charge on the constant potential plate falls to zero. The magnitude of this force maximum is

$$P = P_{\max} = -(2nk_B T) \frac{1}{2} (C_{\max} + 2)$$

$$= (2nk_B T) \{2 \sinh^2(y_{0\infty}/2)\} = \frac{2\pi\sigma_0^2}{\epsilon}. \quad [22]$$

The corresponding separation, d_{\max} , at which this force maximum occurs can be found by the method outlined above. For separations smaller than d_{\max} (double arrows in Fig. 5b), the force will decrease but will remain positive. At $d = 0$, the potentials on the plates will both be equal to $y_{0\infty}$, while the charge on the surfaces will be equal and opposite with magnitude σ_d , so the force approaches the following limit as $d \rightarrow 0$

$$P = (2nk_B T) \left\{ 2 \sinh^2(y_{0\infty}/2) \right\} - \frac{2\pi\sigma_d^2}{\epsilon} = \frac{2\pi(\sigma_0^2 - \sigma_d^2)}{\epsilon}$$

$$= (2nk_B T) \left\{ 2 \sinh^2(y_{0\infty}/2) - 2 \sinh^2(y_{0\infty}/2) \right\}. \quad [23]$$

(ii) Surfaces with Opposite Signs

(1) Surface with higher potential is at constant potential. The movements of the (y, s) coordinates of each surface with decreasing plate separation is given in Fig. 5c. As the plate separation decreases from infinity, the potential on the negative constant charge surface will move toward zero while the charge on the positive constant potential surface will increase (single arrows in Fig. 5c). The force is attractive and has an attractive minimum when the potential on the constant charge surface reaches zero. This attractive minimum is given by

$$P = P_{\min} = -(2nk_B T) \frac{1}{2} (C_{\min} + 2) = -2\pi\epsilon\sigma_d^2. \quad [24]$$

The location of this minimum can be found by the method discussed above. As the separation further decreases, the potential on the constant charge surface will become positive and the charge on the constant potential surface will fall (double arrows in Fig. 5c). The force will become less negative and return to zero at the point where the constant charge curve intersect the curve $\{2 \sinh^2(y_s/2)\}$ at positive potentials. At even smaller separations, the force will become positive and approach the same limit as that given by Eq. [23]. At $d = 0$, the potentials on the plates will both be equal to $y_{0\infty}$, while the charge on the surfaces will be equal and opposite, with magnitude $|\sigma_d|$.

(2) Surface with higher potential is at constant charge. The movements of the (y, s) coordinates of each surface with decreasing plate separation is given in Fig. 5d. As the plate separation decreases from infinity, the potential on the constant charge surface moves toward zero while the charge on the constant potential surface increases in magnitude (single arrows in Fig. 5c). The force is attractive and has an attractive minimum when the potential on the constant charge surface reaches zero. This attractive minimum is given by

$$P = P_{\min} = -(2nk_B T) \frac{1}{2} (C_{\min} + 2) = -2\pi\epsilon\sigma_0^2. \quad [25]$$

The location of this minimum can be found by the method discussed above. As the separation further decreases, the potential on the constant charge surface will become negative and the magnitude of the charge on the constant potential surface will fall (double arrows in Fig. 5d). The force will become less negative but remains negative for all separations. At $d = 0$, where the charge curves intersect, the potentials on the plates will be both equal to $y_{d\infty}$, while the charge

on the surfaces will be equal and opposite, with magnitude σ_0 .

This completes the analysis of the variations of the force, surface charge and/or potentials on each surface as the plate separation changes. This qualitative understanding of the variations as well as knowing the precise values of maxima and minima in the force, potential, and charge is very helpful in implementing and checking numerical calculations of the force and interaction energy in such systems.

THE FREE ENERGY

To calculate the interaction free energy between the plates we require expressions for the free energy change associated with charging up a set of surfaces in contact with a bulk electrolyte of fixed chemical composition by the transfer an amount Γ_j per unit area of ions of type j from the bulk solution to the surface. This can be written generally as (18)

$$F = \int_A dA \sum_j \int_0^{\Gamma_j} (\mu_j^S - \mu_j^B) d\Gamma_j, \quad [26]$$

where μ_j^S and μ_j^B are, respectively, the chemical potentials of ion type j at the surface and in bulk. The summation is over all ions that adsorb on the surface and the integration dA is over all charged surfaces that are in contact with the electrolyte. The chemical potential at the surface can be formally written as

$$\mu_j^S = \bar{\mu}_j^S + v_j e \psi_s, \quad [27]$$

where ψ_s is the mean electrostatic potential on the surface. Combining [26] and [27] we have

$$F = F_{\text{elec}} + F_{\text{chem}} = \int_A dA \int_0^\sigma \psi_s(\sigma) d\sigma$$

$$+ \int_A dA \sum_j \int_0^{\Gamma_j} (\bar{\mu}_j^S - \mu_j^B) d\Gamma_j, \quad [28]$$

where the surface charge density is given by

$$\sigma = \sum_j v_j e \Gamma_j. \quad [29]$$

The interaction free energy at any given separation is then obtained by subtracting off the free energy at infinite separation.

The first term in [28] is identified as the electrical part of the free energy, F_{elec} , and the second term is the chemical contribution, F_{chem} (19). Overbeek has shown that the electrical part of the free energy can be separated into an energetic part and an entropic part (19),

$$F_{\text{elec}} = \int_A dA \int_0^\sigma \psi_s(\sigma) d\sigma = U_{\text{elec}} - T\Delta S_{\text{elec}}, \quad [30]$$

which can in turn be expressed as volume integrals

$$U_{\text{elec}} = \frac{\epsilon}{8\pi} \int_V (\nabla\psi)^2 dV + \frac{\epsilon_p}{8\pi} \int_{V_p} (\nabla\psi)^2 dV_p \quad [31]$$

$$T\Delta S_{\text{elec}} = -\frac{\epsilon}{4\pi} \int_V dV \nabla \cdot (\nabla\psi) + \frac{\epsilon}{4\pi} \int_V dV \int_0^\psi d\psi \nabla \cdot (\nabla\psi). \quad [32]$$

The function $\psi_s(\sigma)$ is the surface potential obtained by solving the Poisson equation for the potential in the electrolyte for given surface charge density σ . The integrals over V are taken over the volume of the electrolyte solution and the integral over V_p is taken over the volumes of the charged particles which have dielectric constant ϵ_p . Equation [31] is the general expression for the electric field energy expressed as an integral over the electric field energy density. The contribution from the field energy inside the particle as represented by the integral over the volume of the particles, was not considered in the earlier work (19) as this contribution can be neglected for constant potential boundary conditions and it makes a small contribution in aqueous systems when $\epsilon \gg \epsilon_p$. In deriving [32] we require the mean potential ψ to obey the Poisson equation: $\nabla^2\psi = -(4\pi/\epsilon)\rho(\psi)$, where the volume charge density, $\rho(\psi)$, in the electrolyte is a general function of the mean potential ψ , but otherwise unspecified. If the Boltzmann distribution is used specifically to relate the mean potential to the volume charge density, the expression for the entropic contribution [32] reduces to (19)

$$T\Delta S_{\text{elec}} = k_B T \int_V dV \sum_i n_{iB} \{ [(v_i e\psi/k_B T) + 1] \times \exp(-v_i e\psi/k_B T) - 1 \}, \quad [33]$$

where n_{iB} is the bulk number density of ions type i with valence v_i . As we shall see, these expressions for the free energy in terms of volume integrals are important in the numerical calculations of the free energy.

Explicit forms for the chemical term

$$F_{\text{chem}} = \int_A dA \sum_j \int_0^{\Gamma_j} (\bar{\mu}_j^S - \mu_j^B) d\Gamma_j \quad [34]$$

depend on how the surfaces acquire their charge. For a constant charge surface, this term is independent of separation since the amount of adsorbed ions on the surface does not change with separation, and therefore this term can be omit-

ted when we evaluate the interaction free energy. Thus the free energy at constant charge becomes

$$F^\sigma = \int_A dA \int_0^\sigma \psi_s(\sigma) d\sigma \quad (\text{constant charge}). \quad [35]$$

For a constant potential surface, we note that at equilibrium $\mu_j^B = \mu_j^S$, so using [27] we have

$$(\bar{\mu}_j^S - \mu_j^B) = -v_j e \psi_s \quad [36]$$

and if ψ_s is held constant, we can use [29] to give

$$F_{\text{chem}} = - \int_A dA \sigma \psi_s. \quad [37]$$

Thus the free energy at constant potential becomes

$$F^\psi = \int_A dA \int_0^\sigma \psi_s(\sigma) d\sigma - \int_A dA \sigma \psi_s \quad [38a]$$

$$= F^\sigma - \int_A dA \sigma \psi_s \quad [38b]$$

$$= - \int_A dA \int_0^{\psi_s} \sigma(\psi) d\psi \quad (\text{constant potential}) \quad [38c]$$

and equation [38b] provides a simple relation between the free energies under constant potential and under constant charge.

For surfaces that acquire their charge through the ionization of surface groups, explicit expressions for F_{chem} have been derived for acidic (18, 20) and amphoteric surfaces (21).

For two interacting flat plates, explicit expressions for the interaction free energy per unit area for constant potential surfaces had been obtained by Devereux and de Bruyn (15). The case of constant charge surfaces can be readily obtained using [38b]. Let $F^\psi(y_0, y_d|d)$ denote the free energy per unit area for constant potential plates. The interaction free energy per unit area, V^{pp} , for the case in which *both* plates are held at constant potential (superscript pp), is then given by

$$\begin{aligned} V^{\text{pp}}(y_0, y_d|d) &= F^\psi(y_0, y_d|d) - F^\psi(y_0, y_d|\infty) \\ &= F^\psi(y_0, y_d|d) + \left(\frac{2nk_B T}{\kappa} \right) \\ &\quad \times \left(\int_0^{y_0} 2 \sinh(y/2) dy + \int_0^{y_d} 2 \sinh(y/2) dy \right) \\ &= F^\psi(y_0, y_d|d) + \left(\frac{2nk_B T}{\kappa} \right) \\ &\quad \times 4 [\cosh(y_0/2) + \cosh(y_d/2) - 2]. \quad [39] \end{aligned}$$

The expressions for $V^{\text{pp}}(y_0, y_d|d)$ differ for the cases (I) $C < -2$, (II) $-2 < C < 2$, and (III) $C > 2$ and we summarize these results in Table 2.

When both surfaces are held at constant charge, the interaction free energy per unit area can be written in terms of V^{pp} using equation [38b]. We denote the interaction free energy per unit area under constant charge by the superscript cc: $V^{\text{cc}}(y_0, y_d|d)$, where y_0 and y_d are the surface potentials at separation d , which are different from the surface potentials of the plates at infinite separation $y_{0\infty}$ and $y_{d\infty}$ because the surface charge densities σ_0 and σ_d are held constant as the separation changes in this case. The connection between the interaction free energy per unit area at constant potential, $V^{\text{pp}}(y_0, y_d|d)$, and that at constant charge, $V^{\text{cc}}(y_0, y_d|d)$, is

$$V^{\text{cc}}(y_0, y_d|d) = V^{\text{pp}}(y_0, y_d|d) + \frac{2nk_{\text{B}}T}{\kappa} \left\{ \sigma_0 [y_0 - y_{0\infty}] - 4[\cosh(y_0/2) - \cosh(y_{0\infty}/2)] + \sigma_d [y_d - y_{d\infty}] - 4[\cosh(y_d/2) - \cosh(y_{d\infty}/2)] \right\}. \quad [40]$$

If only one surface, the one at $\xi = 0$, say, is held at constant potential, that is $y_0 = y_{0\infty}$, the expression for the interaction free energy per unit area will be

$$V^{\text{pc}}(y_0, y_d|d) = V^{\text{pp}}(y_0, y_d|d) + \frac{2nk_{\text{B}}T}{\kappa} \left\{ \sigma_d [y_d - y_{d\infty}] - 4[\cosh(y_d/2) - \cosh(y_{d\infty}/2)] \right\}. \quad [41]$$

The results in [40] and [41] hold for all cases: (I) $C < -2$, (II) $-2 < C < 2$, (III) $C > 2$.

RESULTS FOR SYMMETRIC ELECTROLYTES

We now present numerical results for the variations of the force and interaction free energy per unit area with plate separation. The plates can interact under constant potential or constant charge across a symmetric electrolyte. We will also present results for the variations of the surface potential and surface charge to quantify the descriptions outlined in Figs. 3 to 5. Results are given in terms of the following non-dimensional quantities:

TABLE 2
Interaction Free Energy per Unit Area at Constant Potential

(I) $C \leq -2$	(a) $V^{\text{pp}}(y_0, y_d d) = -\frac{2nk_{\text{B}}T}{\kappa} \left\{ \frac{1}{2} \kappa d [3 \exp(\bar{y}) - 2 - \exp(-\bar{y})] + 2[2 \cosh y_0 - 2 \cosh \bar{y}]^{1/2} - 2[2 \cosh y_d - 2 \cosh \bar{y}]^{1/2} + 4 \exp(\bar{y}/2) [E(k, \phi_0) - E(k, \phi_d)] - 4[\cosh(y_0/2) + \cosh(y_d/2) - 2] \right\}, C \leq -2, \bar{\xi} \geq \kappa d.$
	(b) $V^{\text{pp}}(y_0, y_d d) = -\frac{2nk_{\text{B}}T}{\kappa} \left\{ \frac{1}{2} \kappa d [3 \exp(\bar{y}) - 2 - \exp(-\bar{y})] + 2[2 \cosh y_0 - 2 \cosh \bar{y}]^{1/2} + 2[2 \cosh y_d - 2 \cosh \bar{y}]^{1/2} + 4 \exp(\bar{y}/2) [E(k, \phi_0) + E(k, \phi_d) - 2E(k, \pi/2)] - 4[\cosh(y_0/2) + \cosh(y_d/2) - 2] \right\}, C \leq -2, 0 \leq \bar{\xi} \leq \kappa d.$
	(c) $\bar{y} = \cosh^{-1}(-C/2); k = \exp(-\bar{y}); \phi_0 = \sin^{-1}(\exp([\bar{y} - y_0]/2)); \phi_d = \sin^{-1}(\exp([\bar{y} - y_d]/2)).$
(II) $-2 \leq C \leq 2$	(a) $V^{\text{pp}}(y_0, y_d d) = \frac{2nk_{\text{B}}T}{\kappa} \left\{ -\frac{1}{2} \kappa d [C + 2] + \left(\frac{8[\cosh y_d - 1][\cosh y_d + (C/2)]}{[\cosh y_d + 1]} \right)^{1/2} - \left(\frac{8[\cosh y_0 - 1][\cosh y_0 + (C/2)]}{[\cosh y_0 + 1]} \right)^{1/2} + 4[E(k, \phi_0) - E(k, \phi_d)] + 4[\cosh(y_0/2) + \cosh(y_d/2) - 2] \right\}, -2 \leq C \leq 2, y_d > 0.$
	(b) $V^{\text{pp}}(y_0, y_d d) = \frac{2nk_{\text{B}}T}{\kappa} \left\{ -\frac{1}{2} \kappa d [C + 2] - \left(\frac{8[\cosh y_d - 1][\cosh y_d + (C/2)]}{[\cosh y_d + 1]} \right)^{1/2} - \left(\frac{8[\cosh y_0 - 1][\cosh y_0 + (C/2)]}{[\cosh y_0 + 1]} \right)^{1/2} + 4[2E(k, \pi/2) - E(k, \phi_0) - E(k, \phi)] + 4[\cosh(y_0/2) + \cosh(y_d/2) - 2] \right\}, -2 \leq C \leq 2, y_d < 0.$
	(c) $k = \frac{1}{2}[2 - C]^{1/2}; \phi_0 = \sin^{-1}(1/\cosh(y_0/2)); \phi_d = \sin^{-1}(1/\cosh(y_d/2)).$
(III) $C \geq 2$	(a) $V^{\text{pp}}(y_0, y_d d) = \frac{2nk_{\text{B}}T}{\kappa} \left\{ \frac{1}{2} \kappa d [2 - C] - 2[2 \cosh y_d + C]^{1/2} + 2[2 \cosh y_0 + C]^{1/2} - 4 \exp(y_0/2) \left(\frac{b^{-2} + \exp(y_0)}{b^2 + \exp(y_0)} \right)^{1/2} + 4 \exp(y_d/2) \left(\frac{b^{-2} + \exp(y_d)}{b^2 + \exp(y_d)} \right)^{1/2} + 4b[E(k, \phi_d) - E(k, \phi_0)] + 4[\cosh(y_0/2) + \cosh(y_d/2) - 2] \right\}, C \geq 2, y_d \text{ any sign.}$
	(b) $C = b^2 + b^{-2}; k = \sqrt{1 - b^{-4}}; \phi_d = \tan^{-1}(b \exp(-y_d/2)); \phi_0 = \tan^{-1}(b \exp(-y_0/2)).$

Note. See text for definition of symbols.

$$\text{force per unit area } p = \frac{P}{2nk_B T} \quad [42a]$$

$$\text{interaction free energy per unit area } v = \frac{V}{(2nk_B T/\kappa)} \quad [42b]$$

$$\text{surface potential } y = \frac{ve\psi}{k_B T} \quad [42c]$$

$$\text{surface charge density } s = \frac{4\pi ev}{\kappa\epsilon k_B T} \sigma. \quad [42d]$$

We note that for the interaction between colloidal particles whose radius of curvature a is large compared to the Debye characteristic length, $\kappa a \gg 1$, the Deryaguin construction can be used to calculate the interaction between the spheres from a knowledge of the interaction between parallel plates. In particular, the force, f , between two large spheres of radii a_1 and a_2 with distance of closest approach, h , is

$$f(h) = 2\pi a_H V(h) \quad [43]$$

where

$$\frac{1}{a_H} = \frac{1}{a_1} + \frac{1}{a_2}. \quad [44]$$

In Fig. 6, we show the variations with separation for the force and the interaction energy for two plates that have identical surface potentials when they are at infinite separation: $y_{0\infty} = 2 = y_{d\infty}$. The plates are both held at constant potential (labeled PP), both held at constant charge (CC), and with one surface at constant potential and the other at constant charge (PC). We shall hereafter use the notations CC, PP, and PC to refer to these three types of boundary conditions. One notable feature of the results in Fig. 6 is that the force shows a distinct maximum for the mixed PC boundary conditions at $\kappa d \sim 0.5$. On the other hand, the interaction energy does not exhibit a maximum in this case but attains a maximum at zero separation when the force vanishes. For large separations, the CC and PP cases form, respectively, the upper and lower bounds for the force and energy.

In Fig. 7, we show results for asymmetric plates that can have the same or opposite signs at infinite separation where the surface potentials are $(y_{0\infty}, y_{d\infty}) = (2, \pm 1)$. For the mixed constant charge–constant potential boundary condition, there are now two possibilities distinguished by the two obvious notations: PC($y_{0\infty}, y_{d\infty}$) where the plate at $\xi = 0$ is at constant potential and the plate at $\xi = \kappa d$ is at constant charge; and CP($y_{0\infty}, y_{d\infty}$) which corresponds to constant charge at $\xi = 0$ and at constant potential at $\xi = \kappa d$. Here we see that when the asymmetry is sufficiently large (see also

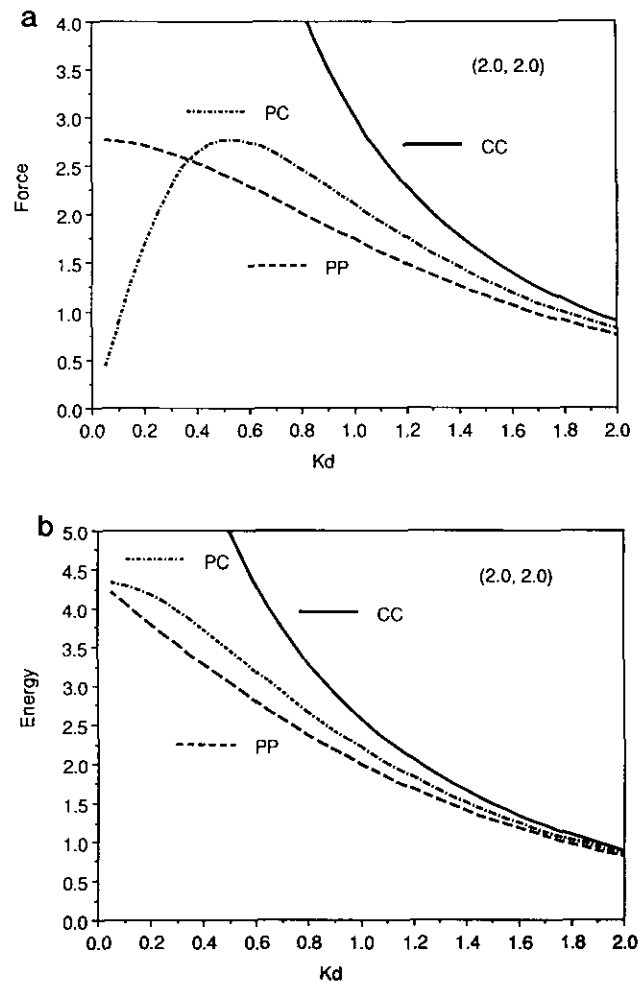


FIG. 6. (a) The nondimensional force and (b) interaction free energy per unit area (see Eq. [42]) between two plates with reduced surface potentials at infinite separation: $y_{0\infty} = 2 = y_{d\infty}$ as a function of the separation, κd , under both surfaces constant potential (PP), both surfaces constant (CC), and one surface at constant potential and the other at constant charge (PC).

Fig. 6), the CC (both plates constant charge) and PP (both plates constant potential) cases form, respectively, the upper and lower bounds for the force and energy for all separations. For separations $\kappa d \sim 1$, the force and energy for the case PC($y_{0\infty}, y_{d\infty}$) is similar to the CC case while that of the CP($y_{0\infty}, y_{d\infty}$) is similar to the PP results. In other words, the behavior of the mixed boundary condition interaction—PC or CP—is largely controlled by the nature of surface whose surface potential is smaller in magnitude. This behavior can be explained by the observation that when two surfaces are in close proximity, the perturbation to the surface with a smaller (in magnitude) potential due to the presence of a high-potential surface is proportionately larger than the perturbation to the surface with the larger potential due to the presence of the low-potential surface. As a consequence the force and energy at large distances are primarily dictated by the way the small potential surface reacts while the large

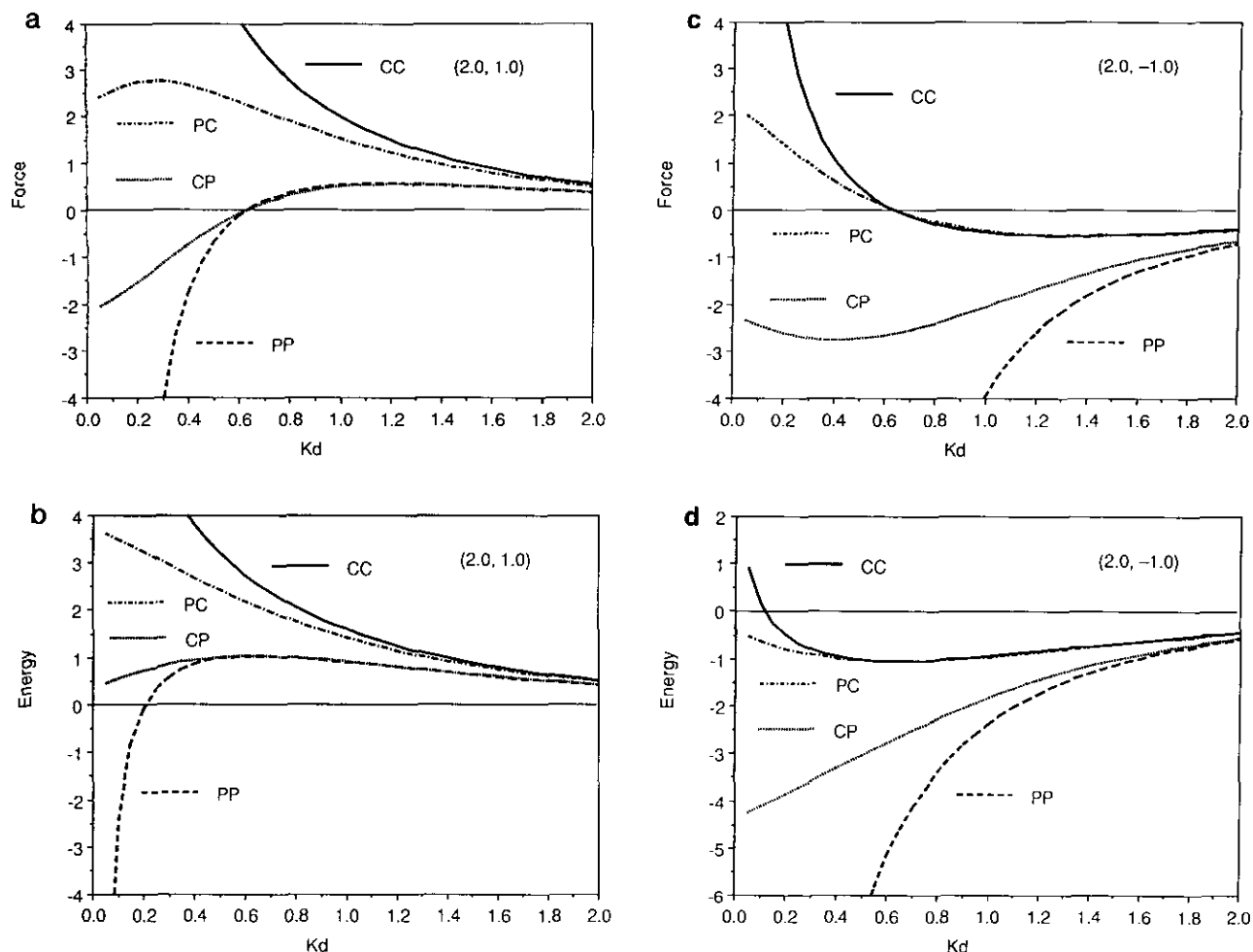


FIG. 7. The force and interaction free energy per unit area between two plates with reduced surface potentials at infinite separation: (a, b) $y_{0\infty} = 2$, $y_{d\infty} = 1$, and (c, d) $y_{0\infty} = 2$, $y_{d\infty} = -1$ as functions of the separation, κd . Labels: CC, both plates at constant charge; PP, both plates at constant potential; PC, the plate at $\xi = 0$ is at constant potential ($y_0 = y_{0\infty}$) and the plate at $\xi = \kappa d$ is at constant charge; CP, the plate at $\xi = 0$ is at constant charge and the plate at $\xi = \kappa d$ is at constant potential ($y_d = y_{d\infty}$).

potential surface remains relatively unperturbed. These remarks are also evident when we examine variations of the surface potential and/or the surface charge with separation shown in Fig. 8.

An interesting feature about the interaction energy between asymmetric surfaces is the presence of a maximum or minimum at separations $\kappa d \sim 1$. In Fig. 9, we show the energy for a set of plates with surface potentials at infinite separation $(y_{0\infty}, y_{d\infty}) = (2, \pm 1)$, $(3, \pm 1)$, $(4, \pm 1)$ under PP or CC conditions. For the PP case, in particular, we note that the location of the maximum of interaction energy per unit area—which is proportional to the measurable force between colloidal particles—moves to larger separation as the asymmetry in potential increases. Since, the maximum can be located at around $\kappa d \sim 1$ or bigger, its presence can be readily detected by direct force measurements. This should be attempted at low ionic strengths, when the maxima will be located at a sufficiently large separation where the influ-

ence of attractive van der Waals forces is less important. An accurate determination of this maximum will also help determine the location of the “origins” of the diffuse layer at each surface. The location of this “origin” relative to physical contact between the surfaces may yield additional information about the extent of any adsorbed layers that may be on the interacting surfaces.

GENERAL ELECTROLYTE AND SURFACE REGULATION

We now consider the interaction between plates that bear ionizable surface groups interacting across a general electrolyte characterized by valencies ν_i and bulk ion number density n_{iB} for species i . We define the quantities

$$\bar{n} \equiv \sum_i n_{iB} \nu_i^2, \quad \beta_i \equiv n_{iB} / \bar{n}, \quad \kappa^2 = \frac{4\pi \bar{n} e^2}{\kappa k_B T} \quad [45]$$

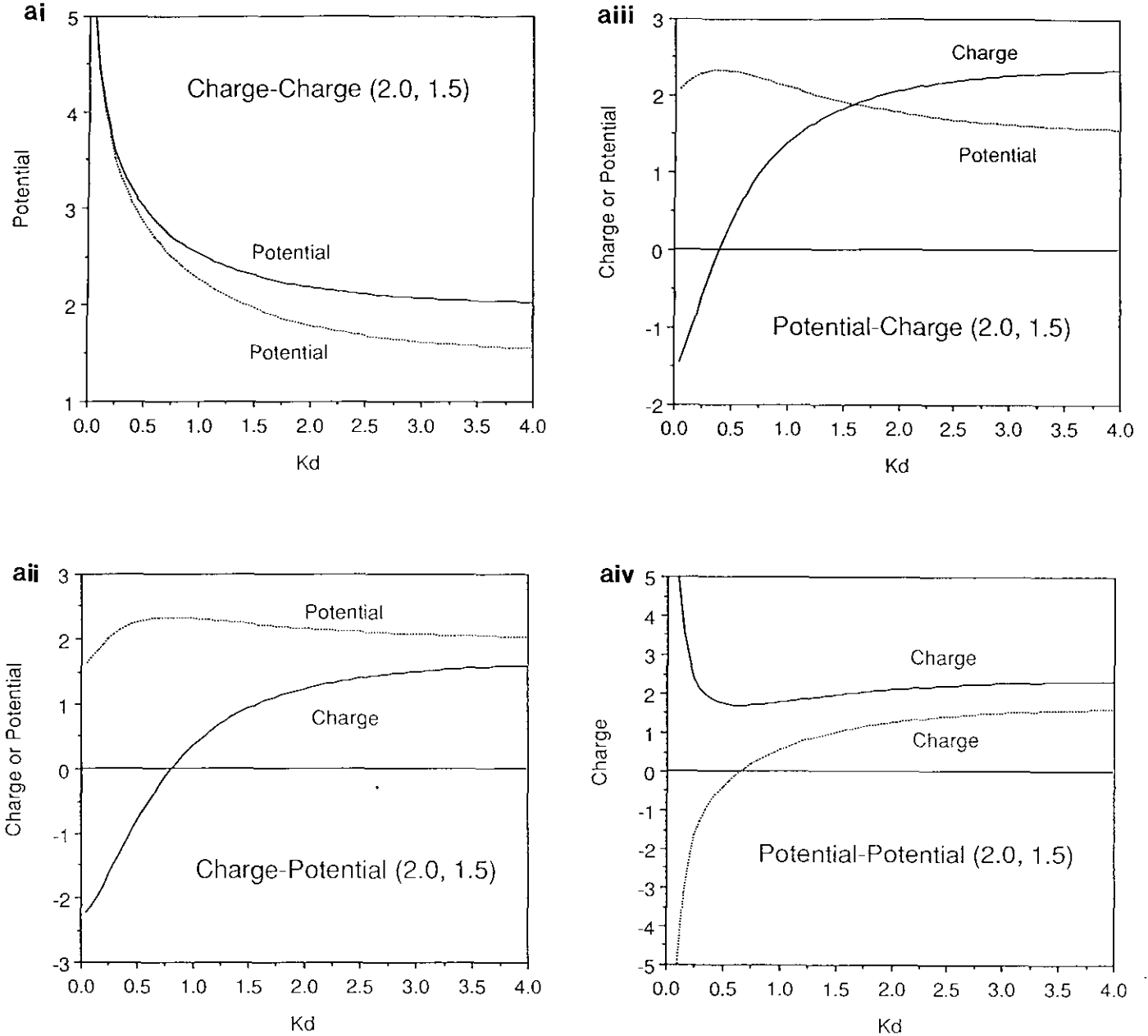


FIG. 8. Variations of nondimensional (see Eq. [42]) surface potential and charge with separation for: (a) $(y_{0\infty}, y_{d\infty}) = (2.0, 1.5)$ and (b) $(y_{0\infty}, y_{d\infty}) = (2.0, -1.5)$ for CC, CP, PC, PP.

so that the general Poisson-Boltzmann equation

$$\frac{d^2\psi(x)}{dx^2} = -\frac{4\pi e}{\epsilon} \sum_i n_{iB} \nu_i \exp(-e\nu_i\psi(x)/k_B T) \quad [46a]$$

can be written in the nondimensional form

$$\frac{d^2\gamma(\xi)}{d\xi^2} = -\sum_i \beta_i \nu_i \exp(-\nu_i \gamma(\xi)) \quad [46b]$$

for which a first integral can be found

$$\left(\frac{d\gamma}{d\xi}\right)^2 = 2 \sum_i \beta_i \exp(-\nu_i \gamma(\xi)) + C. \quad [47]$$

At large separations, $\kappa d \rightarrow \infty$, the condition that both γ and $(d\gamma/d\xi) \rightarrow 0$ as $\xi \rightarrow \infty$, means that

$$C \rightarrow -2 \sum_i \beta_i, \quad \text{as } \kappa d \rightarrow \infty; \quad [48]$$

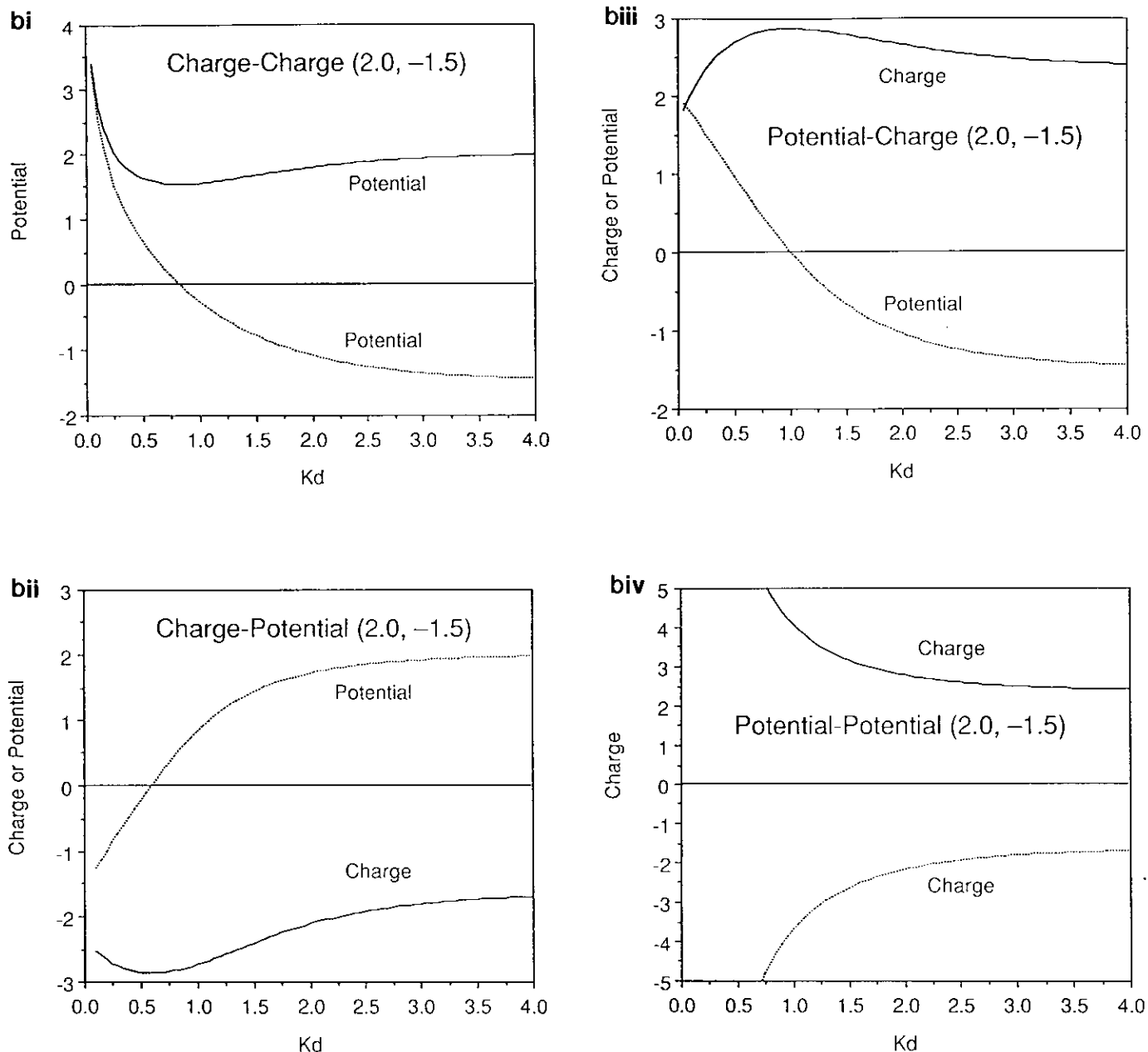


FIG. 8—Continued

therefore in this limit, the charge density is related to the surface potential of an isolated surface, $y_{s\infty}$, by

$$\sigma(\psi) = \frac{\kappa \epsilon k_B T}{4\pi e} \operatorname{sgn}(y_{s\infty}) \left\{ 2 \sum_i \beta_i [\exp(-\nu_i y_{s\infty}) - 1] \right\}^{1/2},$$

$$\kappa d \rightarrow \infty. \quad [49]$$

The constant of integration C is related to the force per unit area by

$$p = P/\bar{n}k_B T = \sum_i \beta_i [\exp(-\nu_i y(\xi)) - 1] - \frac{1}{2} \left(\frac{dy}{d\xi} \right)^2$$

$$= -\frac{1}{2} (C + 2 \sum_i \beta_i). \quad [50]$$

The interaction free energy per unit area, (F/A) , between plates can be obtained from Eq. [28]. However, in this case, we use [30-32] to calculate the electrical contribution because explicit forms for the free energy are not available for a general electrolyte when the plates are at an arbitrary finite

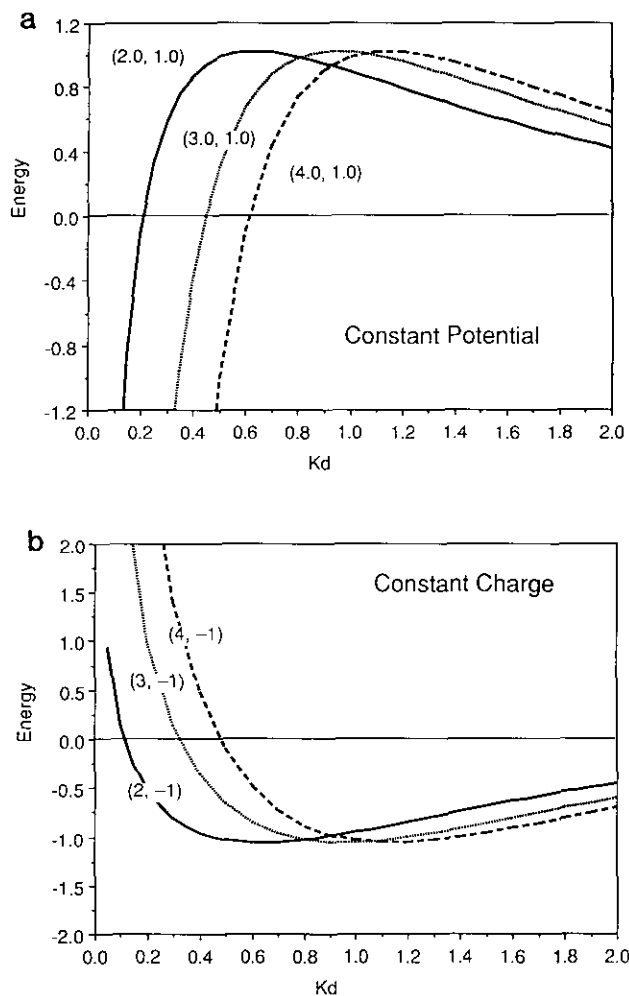


FIG. 9. Nondimensional interaction free energy per unit area for varying degrees of asymmetry (a) at constant potential for both plates with $(y_{0a}, y_{d0a}) = (2, 1)$, $(3, 1)$, and $(4, 1)$ and (b) at constant charge for both plates with $(y_{0a}, y_{d0a}) = (2, -1)$, $(3, -1)$, and $(4, -1)$.

distance apart. The electrical part of the free energy per unit area is

$$F_{\text{elec}}/A = U_{\text{elec}}/A - T\Delta S_{\text{elec}}/A, \quad [51]$$

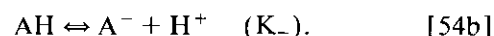
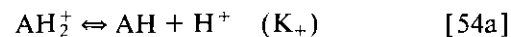
where

$$U_{\text{elec}}/A = \frac{\epsilon}{8\pi} \int_0^d (d\psi/dx)^2 dx \quad [52]$$

$$T\Delta S_{\text{elec}}/A = k_B T \int_0^d dx \sum_i n_{iB} \{ [(\nu_i e\psi/k_B T) + 1] \times \exp(-\nu_i e\psi/k_B T) - 1 \}. \quad [53]$$

In general, these integrals will have to be evaluated numerically.

To obtain expressions of the chemical part of the free energy, we require specific models of how the surfaces acquire their charge by the ionization of surface groups. In this case the boundary conditions need to be modified as neither the charge or potential nor the potential is held constant, but rather the ionization of surface groups imposes a relation between the surface potential and the surface charge at each separation. The surfaces ionization reactions may, for instance, be due amphoteric groups characterized by the reactions:



A mass action treatment of this reaction gives an equation for the surface charge density, $\sigma_s(\psi_s)$ which can be regarded as a function the surface potential, ψ_s (21),

$$\sigma_s(\psi_s) = eN_s \frac{\delta \sinh[e(\psi_N - \psi_s)/k_B T]}{1 + \delta \cosh[e(\psi_N - \psi_s)/k_B T]}, \quad [55]$$

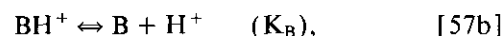
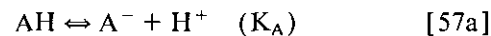
where

$$\delta = 2(K_-/K_+)^{1/2},$$

$$\psi_N = \log(10)(k_B T/e)[(pK_- + pK_+)/2 - \text{pH}] \quad [56]$$

and N_s is the number of amphoteric surface groups per unit area. Equation [55] can be transformed to the equation of state for the charge-potential relation of a surface $s(y_s)$ if we use the scaling given by [42].

If the surface is populated by zwitterionic groups characterized by the reactions



a mass action treatment give the surface charge density, $\sigma_s(\psi_s)$,

$$\sigma_s(\psi_s) = \frac{-eN_A}{1 + (H/K_A)\exp(-e\psi_s/k_B T)} + \frac{eN_B}{1 + (K_A/H)\exp(e\psi_s/k_B T)}, \quad [58]$$

where N_A and N_B are the number of sites of each type per unit area. Equations [55] and [58] express, for the model under consideration, the relationship between the surface charge and the surface potential that must be maintained because of reactions [54] or [57] of the surface groups. We refer to such surfaces generically as regulating surfaces or surface with charge and potential regulation.

Using Eqs. [27] and [36], we can write the chemical part of the free energy per unit area as

$$F_{\text{chem}}/A = \sum_j \int_0^{\Gamma_j} (\bar{\mu}_j^S - \mu_j^B) d\Gamma_j = - \int_0^\sigma \psi_s(\sigma) d\sigma$$

$$= -\sigma_s(\psi_s)\psi_s + \int_{\psi_{\text{pzc}}}^{\psi_s} \sigma_s(\psi) d\psi, \quad [59]$$

where the function $\sigma_s(\psi)$ or $\psi_s(\sigma)$ is the charge-potential relationship due to surface regulation—the equations in [55] and [58] are two specific examples. The lower limit of the last integral, ψ_{pzc} is the value of the potential in the charge-potential relationship for which the surface charge is zero and this limit follows from the lower limit in the $d\sigma$ integral in the preceding line. For the amphoteric model described in [55], $\psi_{\text{pzc}} = \psi_N$; for the zwitterionic model, ψ_{pzc} may be found by setting $\sigma_s(\psi)$ in [58] to zero and solving for $\psi = \psi_{\text{pzc}}$. The free energy under surface regulation, F^r , can now be found from Eqs. [51]–[53] and [59]:

$$F^r/A = F_{\text{elec}}/A + F_{\text{chem}}/A = \frac{\epsilon}{8\pi} \int_0^d (d\psi/dx)^2 dx$$

$$- \int_0^d dx \left\{ \sum_i n_{iB} \nu_i e \exp(-\nu_i e\psi/k_B T) \right\} \psi$$

$$- k_B T \int_0^d dx \sum_i n_{iB} [\exp(-\nu_i e\psi/k_B T) - 1]$$

$$+ \left(-\sigma_s(\psi_s)\psi_s + \int_{\psi_{\text{pzc}}}^{\psi_s} \sigma_s(\psi) d\psi \right)_{\text{surface at } \xi=0}$$

$$+ \left(-\sigma_s(\psi_s)\psi_s + \int_{\psi_{\text{pzc}}}^{\psi_s} \sigma_s(\psi) d\psi \right)_{\text{surface at } \xi=\kappa d}. \quad [60a]$$

The last two terms in brackets are to be evaluated using the charge-potential relations for the surface at $\xi = 0$ and κd , respectively. A geometric interpretation of these results has been given earlier (18, 21). In [60a], the first three integrals over the volume of the electrolyte give partially canceling contributions that result in loss of precision when the integrals are calculated numerically. However, if we use the general form of the Poisson-Boltzmann equation [46a] in the second integral in [60a] and integrate by parts, we obtain the equivalent expression

$$F^r/A = + \left(\int_{\psi_{\text{pzc}}}^{\psi_s} \sigma_s(\psi) d\psi \right)_{\text{surface at } \xi=0}$$

$$+ \left(\int_{\psi_{\text{pzc}}}^{\psi_s} \sigma_s(\psi) d\psi \right)_{\text{surface at } \xi=\kappa d} - \int_0^d \left\{ \frac{\epsilon}{8\pi} (d\psi/dx)^2 \right.$$

$$\left. + k_B T \sum_i n_{iB} [\exp(-\nu_i e\psi/k_B T) - 1] \right\} dx. \quad [60b]$$

This expression for the free energy is numerically more robust since the term in $\{ \}$ is manifestly positive so that numerical evaluation of this integral will not incur loss of significance. Equation [60b] had been obtained earlier in the context of deriving a variational formulation of the free energy (22). This formula will be used for our subsequent calculations.

The second integral of the Poisson-Boltzmann equation cannot be carried out in general for an electrolyte of arbitrary composition. We give a numerical scheme which can handle electrolytes of any composition as well as general nonlinear boundary conditions which arise from regulating surfaces. The scheme is based on Newton-Raphson iterations using Hermite splines to represent the solutions of the Poisson-Boltzmann equation. In this approach, we represent the solution for the potential $y(\xi)$ by a sum of two types of basis functions: $h_j^1(\xi)$ and $h_j^2(\xi)$ in the form

$$y(\xi) = \sum_{j=0}^n [a_{2j+1} h_{j+1}^1(\xi) + a_{2j+2} h_{j+1}^2(\xi)], \quad [61]$$

where the $(2n + 2)$ coefficients (a_1, \dots, a_{2n+2}) are the unknowns to be determined. The details of how this is done is relegated to the Appendix.

This method of solution has the advantage that minimal assumptions are made about the precise form of the Poisson-Boltzmann equation or the boundary conditions so that the method can be used in very general situations. In particular, this is useful for general cases with multicomponent, multivalent electrolyte systems with dissimilar regulating boundary conditions. To test the accuracy of this method, we have repeated the calculations for the constant potential, constant charge and mixed boundary condition cases given in the previous sections. Typically, we can achieve 6 to 7 digits agreement with 10 node points per inverse Debye length. If we use the less robust formula for the free energy in [60a] instead of the preferred formula [60b], we lose 1 to 2 significant figures in the interaction free energy.

To give a simple demonstration of the utility of this method, we present results for the interaction between two dissimilar amphoteric surfaces interacting across a 1:1 electrolyte. The system chosen is unusual in that the force-separation curve exhibits a maximum and a minimum which cannot be observed in any constant charge or constant potential system. The charge-potential curves for our example are given in Fig. 10 and the variations of the force and interaction free energy per unit area with separation are given in Fig. 11. The qualitative variations of the force and interaction free energy with separation shown in Fig. 11 can be readily deduced from the charge potential curves in Fig. 10 using the method of graphical analysis outlined in an earlier section. Due to the very large number of combinations of different variables involved in the interaction between dissimilar surfaces across a general multicomponent, multiva-

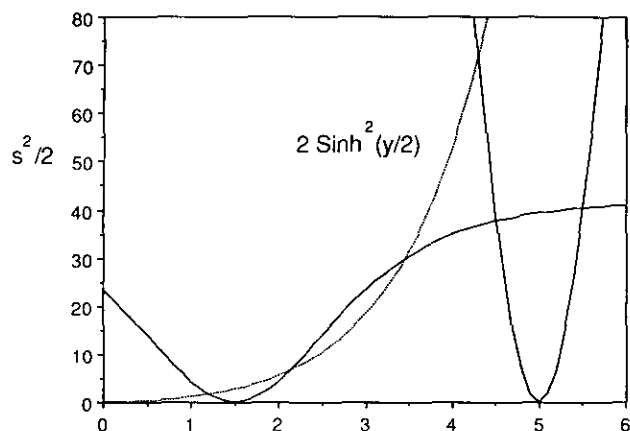


FIG. 10. Charge-potential curves for two dissimilar amphoteric surfaces characterized by the parameters (see Eq. [56]): $(e\psi_{0n}/k_B T) = 5.0$, $(e\psi_{an}/k_B T) = 1.5$, $(e\psi_{0a}/k_B T) = 4.3$, $(e\psi_{aa}/k_B T) = 1.2$ and $\delta = 2.0$ for both surfaces.

lent electrolyte, we shall defer detailed consideration of such system elsewhere.

CONCLUSIONS

We have presented a simple graphical method of analyzing the double-layer interaction between dissimilarly charged surfaces. Numerical results are given for the force and interaction free energy per unit area between such surfaces across a symmetric electrolyte when both surfaces maintain constant surface charge or constant surface potential or, in the mixed case in which one surface is at constant charge and the other at constant potential. In the mixed case, the surface with the smaller magnitude in the surface potential in isolation determines whether the behavior of the interaction is more constant potential-like or constant charge-like. The interaction free energy per unit area between dissimilar planar surfaces exhibits a turning point at $\kappa d \sim 1$. This means that under the Deryagin approximation, the force between colloidal particles will have a similar turning point (Fig. 9). Accurate location by direct force measurement methods may give information about the thickness of any adsorbed layers on the interacting surfaces.

To handle the interaction across multivalent, multicomponent electrolytes as well as charge regulation on dissimilar surfaces due to ionizable groups, we have developed an accurate finite element method of calculating the force and interaction energy in such general cases. The accuracy of this method is the same as the results obtained by more direct methods for interaction across symmetric electrolytes.

APPENDIX

We outline the details of the method of solving the general Poisson-Boltzmann equation using representation [61]. The

interval from $\xi = 0$ to $\xi = \kappa d$ is divided into n intervals of length $\alpha = \kappa d/n$, with $(n + 1)$ equally spaced node points: $(\xi_1 = 0, \xi_2, \dots, \xi_{n+1} = \kappa d)$. With each node point, ξ_k , we associate two basis functions defined by

$$\begin{aligned} h_k^1(\xi) &= -2 \frac{(\xi - \xi_{k-1})^3}{\alpha^3} + 3 \frac{(\xi - \xi_{k-1})^2}{\alpha^2}, & \xi_{k-1} \leq \xi \leq \xi_k \\ &= -2 \frac{(\xi_{k+1} - \xi)^3}{\alpha^3} + 3 \frac{(\xi_{k+1} - \xi)^2}{\alpha^2}, & \xi_k \leq \xi \leq \xi_{k+1} \\ &= 0, & \text{otherwise;} \end{aligned} \quad [A1]$$

$$\begin{aligned} h_k^2(\xi) &= \frac{(\xi - \xi_{k-1})^2(\xi - \xi_k)}{\alpha^2}, & \xi_{k-1} \leq \xi \leq \xi_k \\ &= \frac{(\xi - \xi_k)(\xi_{k+1} - \xi)^2}{\alpha^2}, & \xi_k \leq \xi \leq \xi_{k+1} \\ &= 0, & \text{otherwise.} \end{aligned} \quad [A2]$$

These basis functions are illustrated in Fig. 12. These cubic basis functions have the property that

$$\begin{aligned} h_k^1(\xi) &= 1, & \text{at } \xi = \xi_k \\ &= 0, & \text{at } \xi = \xi_{k-1}, \xi_{k+1} \end{aligned} \quad [A3]$$

$$h_k^2(\xi) = 0, \quad \text{at } \xi = \xi_{k-1}, \xi_k, \xi_{k+1} \quad [A4]$$

and

$$\frac{dh_k^1(\xi)}{d\xi} = 0, \quad \text{at } \xi = \xi_{k-1}, \xi_k, \xi_{k+1} \quad [A5]$$

$$\begin{aligned} \frac{dh_k^2(\xi)}{d\xi} &= 1, & \text{at } \xi = \xi_k \\ &= 0, & \text{at } \xi = \xi_{k-1}, \xi_{k+1}. \end{aligned} \quad [A6]$$

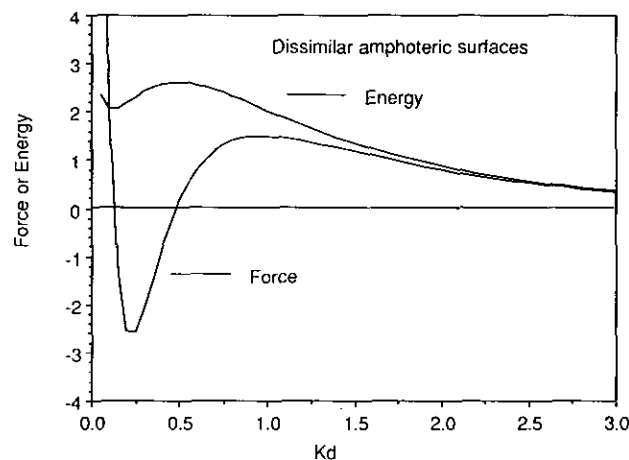


FIG. 11. The nondimensional force and interaction free energy per unit area for two dissimilar amphoteric surfaces characterized by the charge potential curves given in Fig. 10.

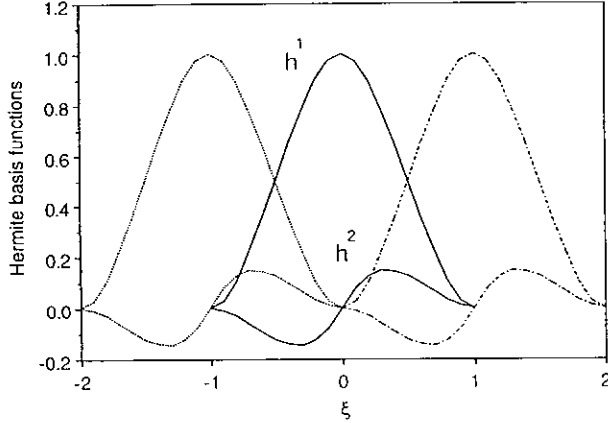


FIG. 12. Hermite cubic basis functions $h^1(\xi)$ and $h^2(\xi)$ given by Eqs. [A1] and [A2] as used in representing the solution of the Poisson–Boltzmann equation with the interval $\alpha = 1$ (solid curves). The two sets of broken curves represent basis functions centred about the neighboring nodes.

From these properties of the cubic basis functions, we now see that the odd coefficients, a_{2k+1} , in representation [61] for the potential $\psi(\xi)$ are approximations to the *value* of the potential at $\xi = \xi_k$, while the even coefficients, a_{2k} , are approximations to the *derivative* of the potential at the same point. This representation is different from a finite difference scheme in that the both the potential and its first derivative are calculated to the same order of accuracy. This is important because we intend to use Eq. [60] to calculate the free energy which involves both the potential and its derivative. The truncation error in this representation in terms of cubic basis functions is of order α^5 (where α is the discretization step size) for the function and the derivative, whereas a typical second-order finite difference scheme will have errors of order α^3 in the function and errors order α^2 in the derivative. This means that the truncation error is much smaller in our scheme. Further, function and derivative values in between grid points can be computed using the cubic basis functions to the same order of accuracy, while a finite difference scheme will require further interpolation between the grid points. This feature is important as we need to evaluate the integrals in [60] for the free energy as accurately as possible. The coefficients $\{a_k\}$ can be found by requiring the representation [61] to satisfy the Poisson–Boltzmann equation plus the given boundary conditions.

The general nondimensional Poisson–Boltzmann Eq. [46] can be written in the form

$$\frac{d^2 y(\xi)}{d\xi^2} = f(y). \quad [\text{A7}]$$

Suppose $\psi(\xi)$ is approximated by $u(\xi)$ so that

$$\psi(\xi) = u(\xi) + \delta u(\xi), \quad [\text{A8}]$$

where the correction term $\delta u(\xi)$ is small ($|\delta u(\xi)| \ll |\psi(\xi)|$). Then combining [A7] and [A8] and expanding to first order in $\delta u(\xi)$, we have

$$\frac{d^2 y}{d\xi^2} = f(u) + (y - u)f'(u) + O(\delta u)^2, \quad [\text{A9}]$$

so that if $u(\xi)$ is a known approximation to the solution of [A7], Eq. [A9] can be solved to give a better estimate, namely $\psi(\xi)$. Call this new estimate $u_{n+1}(\xi)$ and the previous estimate $u_n(\xi)$, the Newton–Raphson iterations scheme involves discarding the term proportional to $(\delta u)^2$ and solving the following *linear* differential equation for the new estimate u_{n+1}

$$\frac{d^2 u_{n+1}}{d\xi^2} - u_{n+1} f'(u_n) = f(u_n) - u_n f'(u_n) \quad [\text{A10}]$$

given a previous estimate $u_n(\xi)$.

Similarly, the nonlinear boundary condition at a regulating surface, which has the general form

$$\frac{dy(\xi)}{d\xi} = g(y), \text{ on a surface,} \quad [\text{A11}]$$

can be linearized as

$$\begin{aligned} \frac{du_{n+1}}{d\xi} - u_{n+1} g'(u_n) \\ = g(u_n) - u_n g'(u_n), \text{ on a surface.} \end{aligned} \quad [\text{A12}]$$

Assuming that $u_n(\xi)$ is known, we can find the coefficients $\{a_k, k = 1, \dots, (2n+2)\}$ in [61], by substituting the series [61] for $u_{n+1}(\xi)$ into [A10], and requiring this series to satisfy the linear differential equation at the following collocation points

$$\frac{(\xi - \xi_1)}{\alpha} = \frac{1}{\sqrt{3}}, \quad \frac{(\xi - \xi_{n+1})}{\alpha} = -\frac{1}{\sqrt{3}}, \quad [\text{A13a}]$$

$$\frac{(\xi - \xi_k)}{\alpha} = \pm \frac{1}{\sqrt{3}}, \quad \text{for } k = 2, \dots, n. \quad [\text{A13b}]$$

This gives $2n$ equations. Two more equations can be obtained by applying the boundary condition [A12] on each surface. This gives $(2n+2)$ linear equations for the same number of unknowns. The resultant coefficient matrix is a banded matrix with bandwidth 4 and can be solved by standard methods. The iteration based on Eqs. [A10] and [A12] is repeated until convergence is obtained. The Newton–Raphson scheme gives quadratic convergence and usually less than five iterations are required.

GLOSSARY

C	integration constant, [6]
d	plate separation
e	protonic charge
$E(k, \phi)$	incomplete elliptic integral of the second kind of modulus k and amplitude ϕ
f	free energy
$F(k, \phi)$	incomplete elliptic integral of the first kind of modulus k and amplitude ϕ
k	modulus of elliptic integrals
$K(k)$	complete elliptic integral of the second kind of modulus k
k_B	Boltzmann constant
n	bulk ion number density
\bar{n}	mean bulk ion number density, [45]
P	pressure between plates
p	nondimensional pressure, [42]
s	nondimensional surface charge density, [42]
T	absolute temperature
V	interaction free energy per unit area between parallel plates
v	nondimensional interaction free energy per unit area, [42]
x	coordinate normal to the plate
$y(\xi)$	nondimensional potential [42]
\bar{y}	nondimensional potential at the minimum in the electrostatic potential curve
β	ionic fraction [45]
ϵ	dielectric constant or relative permittivity
ϕ	amplitude of elliptic integrals
κ	Debye screening parameter, [45]
ν	ionic valence
σ	surface charge density
ξ	nondimensional coordinate normal to the surface, κx
ξ_d	nondimensional plate separation, κd
$\bar{\xi}$	location of the minimum in the electrostatic potential curve
ψ	electrostatic potential
μ_j	chemical potentials, see [26]

Superscripts

C	at constant charge
P	at constant potential
CC	both surfaces at constant
CP	surface at $x = 0$ is at constant charge; surface at $x = d$ is at constant potential
PC	surface at $x = 0$ is at constant potential; surface at $x = d$ is at constant charge
PP	both surfaces at potential

Subscripts

B	quantity evaluated in the bulk electrolyte
d	quantity evaluated at the surface at $x = d$

i	index for ionic species i
0	quantity evaluated at the surface at $x = 0$
∞	quantity pertaining to the large separation limit, $d \rightarrow \infty$

ACKNOWLEDGMENT

This work has been supported in part by the Advanced Mineral Processing Centre, a Special Research Centre funded by the Australian Federal Government at the University of Melbourne. Financial support from the Australian Research Council to D.Y.C. and S.L.C. is gratefully acknowledged.

REFERENCES

1. Isrealachvili, J. N., and Adams, G., *J. Chem. Soc. Faraday Trans. 1* **74**, 975 (1978).
2. Ducker, W. A., Senden, T. J., and Pashley, R. M., *Nature* **353**, 239 (1991); *Langmuir* **8**, 1831 (1992).
3. Atkins, D. T., and Pashley, R. M., *Langmuir* **9**, 2232 (1993); Grabbe, A., and Horn, R. G., in "Proceedings of the NATO Advanced Research Workshop on Clay Swelling and Expansive Soils" (P. Baveye and M. B. McBride, Eds.). Kluwer Academic, in press.
4. Verwey, E. J. W., and Overbeek, J. Th. G., "Theory of the Stability of Lyophobic Colloids." Elsevier, New York, 1948.
5. Deryaguin, B. V., *Kolloid Z.* **69**, 155 (1934).
6. Honig, E. P., and Mul, P. M., *J. Colloid Interface Sci.* **36**, 258 (1971).
7. Usui, S., *J. Colloid Interface Sci.* **44**, 107 (1973).
8. Gregory, J., *J. Chem. Soc. Faraday II* **69**, 1723 (1973); *J. Colloid Interface Sci.* **51**, 44 (1975).
9. Hogg, R. T., Healy, T. W., and Fuerstenau, D. W., *Trans. Faraday Soc.* **62**, 1638 (1966).
10. Bierman, A., *J. Colloid Sci.* **10**, 231 (1955).
11. Ohki, S., *J. Colloid Interface Sci.* **37**, 318 (1971).
12. Usui, S., *J. Colloid Interface Sci.* **97**, 247 (1984).
13. Parsegian, V. A., and Gingell, D., *Biophys. J.* **12**, 1192 (1972).
14. Carnie, S. L., and Chan, D. Y. C., *J. Colloid Interface Sci.* **161**, 260 (1993).
15. Devereux, O. F., and de Bruyn, P. L., "Interaction of Plane Parallel Double Layers." MIT Press, Cambridge, 1963.
16. Bell, G. M., and Peterson, G. C., *J. Colloid Interface Sci.* **41**, 542 (1972).
17. Ohshima, H., *Colloid Polymer* **252**, 158 (1974); **252**, 257 (1974); **253**, 150 (1975).
18. Chan, D. Y. C., and Mitchell, D. J., *J. Colloid Interface Sci.* **95**, 193 (1983).
19. Overbeek, J. Th. G., *Colloids Surf.* **51**, 61 (1990).
20. Payens, Th. A. J., *Philips Res. Rep.* **10**, 425 (1955).
21. Chan, D. Y. C., in "ACS Symposium Series" (Davis, J. A., and Hayes, K. F., Eds.). Vol. 323, p. 99, 1986.
22. Reiner, E. S., and Radke, C. J., *J. Chem. Soc. Faraday Trans.* **86**, 3901 (1990).
23. Reiner, E. S., and Radke, C. J., *J. Adv. Colloid Interface Sci.* **47**, 59 (1993).
24. Krozal, J. W., and Saville, D. A., *J. Colloid Interface Sci.* **150**, 365 (1992).
25. We have explicitly considered the interaction between infinitely thick plates. When the plates have finite thickness, we also need to specify the plate dielectric constant as an additional parameter. For constant potential boundary conditions, the plate properties are irrelevant. For other boundary conditions, the properties of the plate will affect the asymptotic form of the force as the separation $d \rightarrow 0$. However, if our results are to be used with the Deryaguin approximation to calculate the interaction between colloidal particles, then results from the interaction between infinitely thick plates should be used.